ICES Journal of Marine Science, 2023, **00**, 1–19
DOI: 10.1093/icesjms/fsad104
Original Article

Characterizing coastal cod vocalization using a towed hydrophone array

Sai Geetha Seri [1], Matthew Edward Schinault [1], Seth Michael Penna [1], Chenyang Zhu [1], Lise Doksæter Sivle [2], Karen de Jong [2], Nils Olav Handegard [2], and Purnima Ratilal [1,*]

[1]Laboratory for Ocean Acoustics and Ecosystem Sensing, Northeastern University, Boston, MA 02115, USA
[2]Institute of Marine Research, Nordnes, N-5817 Bergen, Norway

*Corresponding author: tel: +1-617-373-8458; e-mail: purnima@ece.neu.edu.

To better understand spawning vocalizations of Norwegian coastal cod (*Gadus morhua*), a prototype eight-element coherent hydrophone array was deployed in stationary vertical and towed horizontal modes to monitor cod sounds during an experiment in spring 2019. Depth distribution of cod aggregations was monitored concurrently with an ultrasonic echosounder. Cod vocalizations recorded on the hydrophone array are analysed to provide time–frequency characteristics, and source level distribution after correcting for one-way transmission losses from cod locations to the hydrophone array. The recorded cod vocalization frequencies range from ∼20 to 600 Hz with a peak power frequency of ∼60 Hz, average duration of 300 ms, and mean source level of 163.5 ± 7.9 dB re 1 μPa at 1 m. Spatial dependence of received cod vocalization rates is estimated using hydrophone array measurements as the array is towed horizontally from deeper surrounding waters to shallow water inlet areas of the experimental site. The bathymetric-dependent probability of detection regions for cod vocalizations are quantified and are found to be significantly reduced in shallow-water areas of the inlet. We show that the towable hydrophone array deployed from a moving vessel is invaluable because it can survey cod vocalization activity at multiple locations, providing continuous spatial coverage that is complementary to fixed sensor systems that provide continuous temporal coverage at a given location.

Keywords: cod, detection range, fish grunts, fish knocks, hydrophone array and probability of detection, passive ocean acoustic waveguide remote sensing, source level, time–frequency characterization, vocalization rates.

Introduction

Coastal cod (*Gadus morhua*) is a commercially valuable fish species and an important constituent of Norwegian coastal ecosystems (Vølstad *et al.*, 2011; Kleiven *et al.*, 2016). Understanding cod behaviour, including sound production and communication, especially during the spawning season is essential to species management (Sund, 1935). During the spawning season, cod gather in large spawning aggregations that have been mapped locally over the water-column depth for decades using conventional ultrasonic fisheries echosounder across the Norwegian coast (Morgan *et al.*, 1997; Nordeide and Båmstedt, 1998; Ermolchev, 2009; Ingvaldsen *et al.*, 2017). More recently, cod shoals have been imaged over instantaneous wide areas using waveguide-based acoustic imaging technology (Makris *et al.*, 2019) to reveal large-scale distributions in the Norwegian and Barents Seas.

Previous passive acoustic studies of Atlantic cod vocalizations have been based on observations with a single hydrophone either fixed (Finstad and Nordeide, 2004; Caiger *et al.*, 2020) or deployed from autonomous gliders (Zemeckis *et al.*, 2019). Some studies have also been based on captured cod housed in a tank (Brawn, 1961; Wilson *et al.*, 2014) or in large net enclosures (Vester *et al.*, 2004). It was found that cod grunts are produced either due to aggressive behaviour by both sexes or during the spawning period by males (Brawn, 1961). It was observed that males with larger drumming muscles produce louder sounds (Rowe and Hutchings, 2004). The lack of an in-depth description of cod sounds in these earlier studies prompted further work, which expanded upon the reproductive behaviour of cod. Several studies of tagged cod (Cote *et al.*, 2004; Robichaud and Rose, 2004; Lindholm *et al.*, 2007; Skjæraasen *et al.*, 2011) have been conducted to reveal cod behaviour, movement, and migration patterns over time, including wide sections of the North Atlantic range of cod fish.

Here, the observation and analysis approach for cod vocalizations follows the passive ocean acoustic waveguide remote sensing (POAWRS) technique (Ratilal *et al.*, 2022), but for measurements made using a short eight-element prototype coherent hydrophone array (Schinault *et al.*, 2019). The POAWRS technique was previously developed and implemented for a much larger 160-element coherent hydrophone array system where POAWRS was applied to detect, characterize, and localize acoustic signals from various underwater sound producers, such as marine mammal vocalization signals from both baleen and toothed whale species (Gong *et al.*, 2014; Tran *et al.*, 2014; Huang *et al.*, 2016; Wang *et al.*, 2016a; Garcia *et al.*, 2018), as well as tonal and broadband amplitude modulated cyclostationary signals generated by surface ships (Huang *et al.*, 2017; Zhu *et al.*, 2018). Here, we demonstrate that the POAWRS approach can be useful for passive acoustic monitoring of fish spawning activities by passive acoustic detection of fish sounds.

The coastal cod vocalizations analysed here were recorded in a coastal spawning habitat at Austevoll, western Norway. The area is a known spawning ground where cod fish have been tagged, tracked, and studied over multiple years (e.g.

Received: 29 September 2022; **Revised:** 10 May 2023; **Accepted:** 25 May 2023
© The Author(s) 2023. Published by Oxford University Press on behalf of International Council for the Exploration of the Sea. This is an Open Access article distributed under the terms of the Creative Commons Attribution License (https://creativecommons.org/licenses/by/4.0/), which permits unrestricted reuse, distribution, and reproduction in any medium, provided the original work is properly cited.

Downloaded from https://academic.oup.com/icesjms/advance-article/doi/10.1093/icesjms/fsad104/7218794 by guest on 09 August 2023

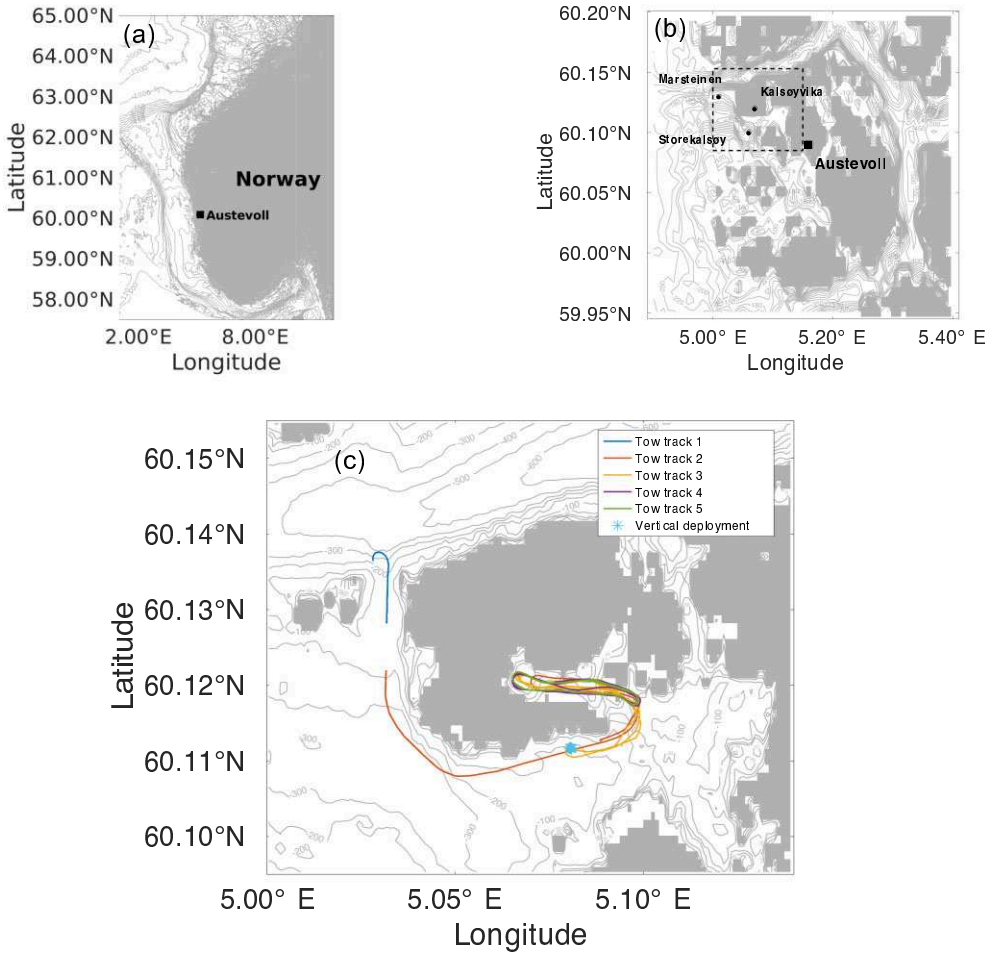

Figure 1. (a, b) Observation region of the experiment deploying an eight-element hydrophone array from 6 to 8 March 2019. (c) The survey data analysis is subdivided into six distinct segments corresponding to different days and times, as well as mode of array deployment. Stationary (light blue star) represents the GPS location of the vertically deployed hydrophone array on 7 March 2019. Track details for the horizontally towed hydrophone array are provided in Table 1.

Table 1. Overview of the survey conducted in the Austevoll region from 6 to 8 March 2019.

Date	Time start	Time stop	Single hydrophone or array	Type (towed, stationary)
6 March 2019	17:07	18:32	B&K hydrophone pair	Stationary vertical
7 March 2019	14:29	14:46	B&K hydrophone pair and array deployed simultaneously	Stationary vertical
7 March 2019	12:54	13:02	Array	Towed—track 1
7 March 2019	13:07	14:09	Array	Towed—track 2
7 March 2019	14:57	17:02	Array	Towed—track 3
8 March 2019	13:27	14:27	Array	Towed—track 4
8 March 2019	15:51	16:47	Array	Towed—track 5

Skjæraasen *et al.*, 2011; McQueen *et al.*, 2022, 2023). Using an acoustic telemetry locating system, McQueen *et al.* (2023) investigated the potential effects of seismic airgun surveys on cod behaviour during spawning, examining swimming depth, swimming acceleration, displacement, and area. Meager *et al.* (2012) investigated the influence of environmental factors, such as temperature and wind, on the depth-related behaviour of cod at a spawning site. Passive acoustic monitoring, as opposed to tagged studies, will be important in identifying how external factors impact cod communication during spawning, since acoustic communication is a potential method for cod mate assessment (Nordeide and Kjellsby, 1999; Rowe and Hutchings, 2006).

Here, analysis is conducted for acoustic data from the eight-element coherent hydrophone array, as well as a pair of Brüel & Kjær (B&K) hydrophones, deployed to monitor cod sounds at Austevoll in spring 2019. The observations were made to coincide with the cod spawning season for that region. The eight-element array was deployed in both stationary vertical and towed horizontal modes. Depth distributions of coastal cod aggregations were monitored concurrently using a hull-mounted ultrasonic echosounder. Concurrent

Downloaded from https://academic.oup.com/icesjms/advance-article/doi/10.1093/icesjms/fsad104/7218794 by guest on 09 August 2023

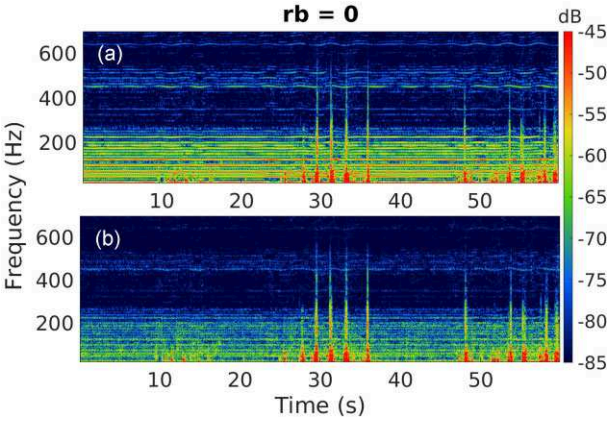

Figure 2. (a) Power spectrogram density of measured coastal cod vocalizations in units of dB re 1 V^2/Hz obtained after coherent beamforming in broadside direction (relative bearing, $rb = 0$) of a vertically deployed eight-element hydrophone array. (b) Output after time-differencing of the beamformed spectrogram, significantly reduced the intensity of ship tonal signals, thus enhancing detection of impulsive cod grunt signals.

positioning information for tagged cod in the shallow-water bay at Austevoll further confirms the presence of cod fish during this study.

The passive acoustic data recordings are analysed to provide detection, time–frequency characterization, and spatial and source level distributions of received cod vocalizations. The source level distribution of received cod vocalizations, back-projected to a distance of 1 m from the fish, is estimated by correcting for transmission losses in the water column. The spatial dependence of cod vocalization detection rate along designated tracks in the region traversing the shallow-water bay inlet and deeper surrounding areas is determined from measurements of the towed hydrophone array. Further insights into cod spatial distribution are provided by the probability of detection (PoD) region calculation for Norwegian coastal cod vocalizations in both the shallow-water bay inlet and deeper surrounding areas at Austevoll with the hydrophone array as receiver. The PoD region for a given percentage, P%, is a region of space surrounding the receiver where the probability of detecting a given source, in this case, vocalizing cod, is $\geq P/100$. The PoD region is calculated via the passive sonar equation taking into account the measured statistical source level distribution, ambient noise level distribution, potential beamforming array gain enhancement, detection threshold, and range- and azimuth-dependent transmission loss modelling in an ocean waveguide.

An eight-element hydrophone array is used here to passively detect and understand the baseline behaviour of cod vocalizations. Since cod is highly vocal during spawning (Rowe and Hutchings, 2006; Caiger *et al.*, 2020; Hawkins, 2022), passive acoustic monitoring of their vocalizations can be used to infer their temporo-spatial distributions, dynamics, and behaviour. Here, we demonstrate that a short eight-element hydrophone array towed from a mobile platform provides an efficient and versatile approach for studying the spatial dependence of fish vocalizations in near real time at various locations with bathymetric variations, such as shallow bay inlets areas where water depths are typically <30 m, as well as surrounding slope and deeper water areas roughly 300 m deep. This study is not intended to survey the entire spawning habitat for cod, but to examine the methods and possibility for mapping spawning habitats with a towable hydrophone array.

Material and methods

Experiment, instrumentation, and acoustic data collection

The cod vocalizations analysed here were recorded during an experiment from 6 to 9 March 2019 in a bay in Austevoll, western Norway (Figure 1). This experiment is part of a research project (SpawnSeis, NFR grant number 280367) by the Institute of Marine Research (IMR), Norway. The project goal is to understand how seismic surveys with airgun sound sources affect the spawning behaviour of cod, and to do so, a good understanding of their natural behaviour, hereunder vocal behaviour, is needed. The prototype eight-element coherent hydrophone array (Schinault *et al.*, 2019) developed by Northeastern University was included as part of this study to record and survey cod vocalizations in a shallow bay in Austevoll and deeper surrounding waters. The array provides an efficient approach for surveying a larger area via towed sensors on a mobile platform than observations made with a single stationary hydrophone.

The experimental site in Austevoll, which is outside Bergen, Norway (see Figure 1), includes the shallow inlet of Kalsøyvika and deeper waters around Storakalsøy and Marsteinen. In this experiment, recordings of underwater sound were acquired using three different set-ups deployed from RV Hans Brattstrøm: (a) a pair of vertically deployed B&K hydrophones spaced 1 m apart with the shallowest at 14 m depth on 6 March 2019, (b) a vertically deployed eight-element hydrophone array with the shallowest hydrophone at 10 m depth alongside the pair of B&K hydrophones with simultaneous acquisition on 7 March 2019, and (c) the horizontally deployed eight-element hydrophone array towed along designated tracks (see Figure 1) at an average speed of 4 knots (roughly 2 m s^{-1}) on 7 and 8 March 2019. A summary of the sensors deployed is provided in Table 1, including date, time, and type of deployment. The data acquired by the horizontally towed hydrophone array are divided into five different segments (or tracks) over 2 d. To minimize the effect of tow ship noise on the recorded acoustic data, the hydrophone array was towed ~60–80 m behind the research vessel, given a maximum tow cable length of 100 m.

The eight-element coherent hydrophone array has 0.75 m spacing for spatially unaliased beamforming up to 1000 Hz for narrowband signals. The array gain is dependent on the signal frequency and bearing with up to $10\log_{10}(N) = 9$ dB, where N is the number of hydrophones. The actual array gain, which may be <9 dB theoretical array gain, is dependent on noise coherence and cod vocalization wavelength relative to array aperture length. The sampling frequency for the array is adjustable and can be set at either 8, 30, or 100 kHz per channel. The data analysed here were recorded at 8 kHz sampling frequency, which is sufficient for cod sounds. The B&K hydrophone type 8106 is a wide-range, general-purpose transducer for making sound measurements over a frequency range from 7 Hz to 80 kHz with a receiving sensitivity of -174 dB re 1 V/μPa. It features a built-in, thick-film, and

Downloaded from https://academic.oup.com/icesjms/advance-article/doi/10.1093/icesjms/fsad104/7218794 by guest on 09 August 2023

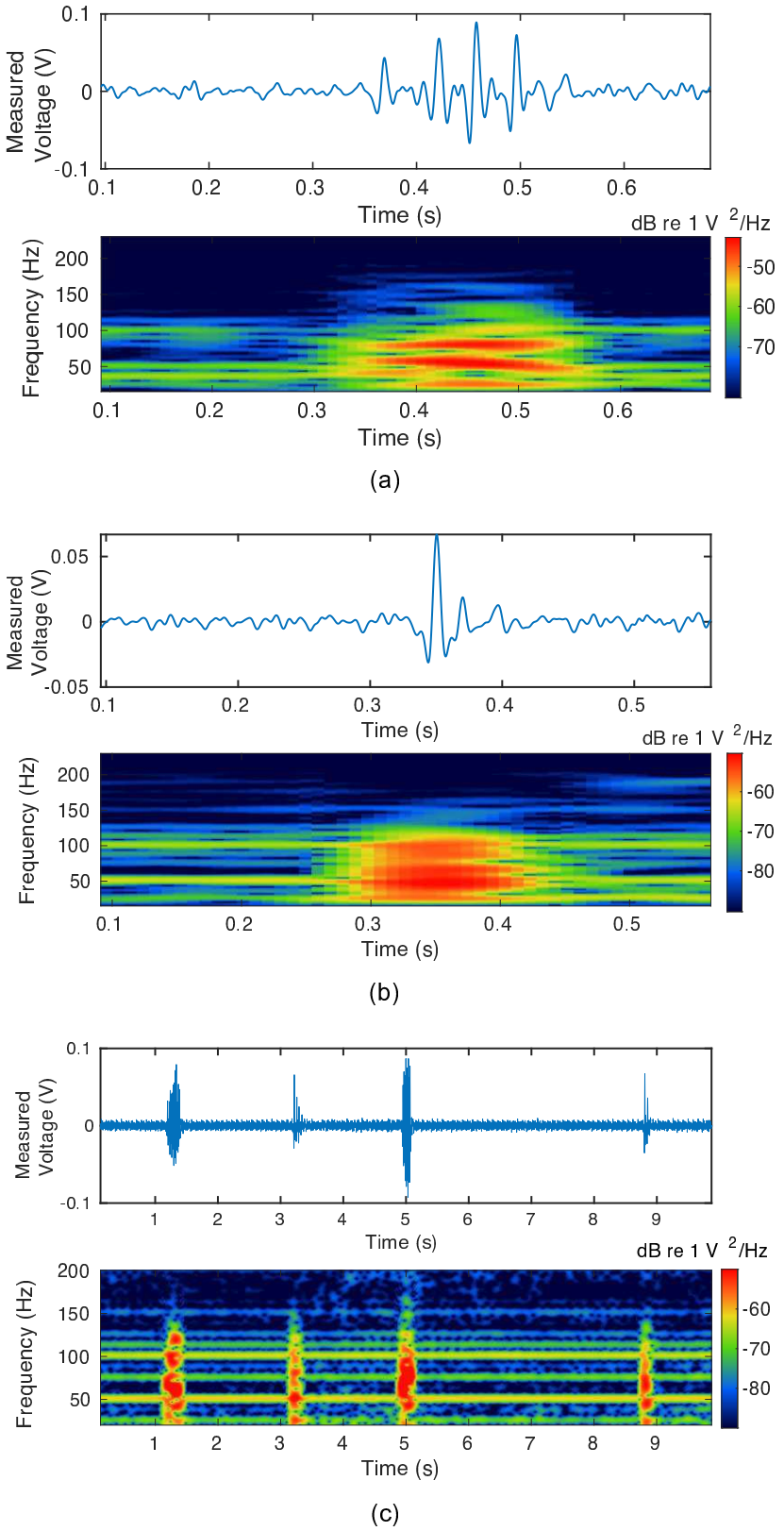

Figure 3. Time domain and spectrogram of (a) coastal cod grunt, (b) coastal cod knock, and (c) a series of coastal cod vocalizations. The above vocalizations were recorded on both B&K hydrophones deployed vertically on 6 March 2019, and shown here for one of the hydrophones.

Downloaded from https://academic.oup.com/icesjms/advance-article/doi/10.1093/icesjms/fsad104/7218794 by guest on 09 August 2023

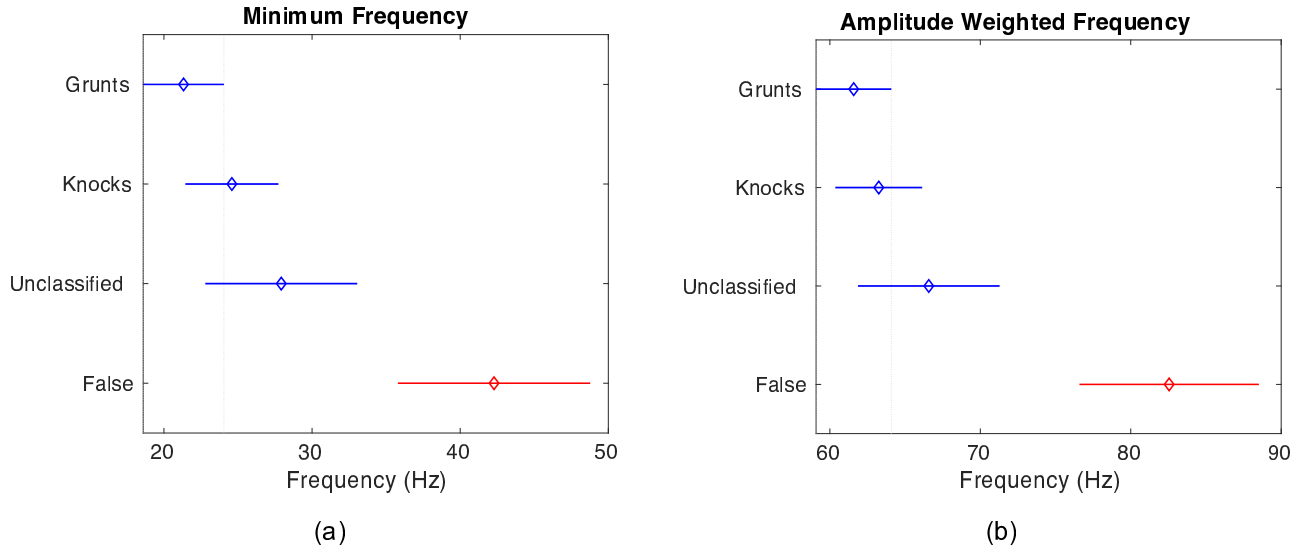

Figure 4. Results of one-way ANOVA analysis to compare the frequency characteristics of all 388 shortlisted detections received on a B&K hydrophone. Time–frequency characteristics of four sub-classes "cod grunts", "cod knocks", "cod unclassified", and "false detections" were considered. The blue and red circles indicate the mean of respective classes. The blue and red bars represent the confidence intervals for those classes. Classes that do not have significantly different means appear in blue. From (a) minimum frequencies and (b) power amplitude weighted frequencies, it can be observed that false detections have significantly different characteristics.

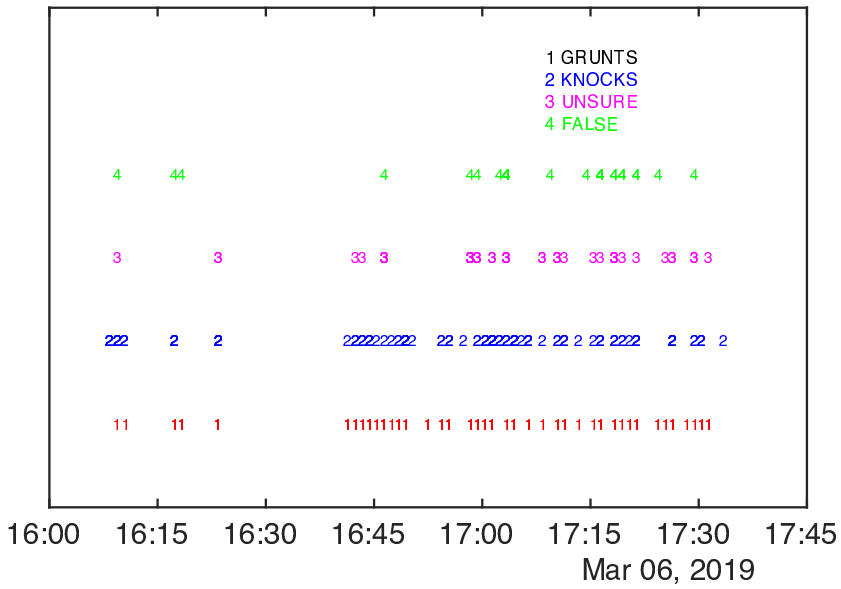

Figure 5. Time grouping of the 388 shortlisted signals recorded on the single B&K Hydrophone on 6 March 2019. This grouping indicates that the different types of vocalizations occurred simultaneously.

low-noise 10 dB preamplifier for signal conditioning (Types, 1992). The eight-element hydrophone array measurements are compared to the B&K hydrophone measurements for calibration.

The research vessel Hans Brattstrøm was also equipped with a Simrad EK60 echo sounder configured with a split-beam transducer (*ES*38—12) having a nominal 12° beamwidth for surveying the water column directly underneath the research vessel. The water-column temperature and conductivity were sampled using a conductivity–temperature–depth (CTD) sensor (SAIV sonde SD208) at the shallow-water inlet Kalsøyvik and deeper Marstein area. The water depth at the shallow-inlet Kalsøyvik site ranged from 16 to 78 m with an average of ~50 m, while the water depth in the outer region surrounding Storakalsøy and Marstein ranged from ~100 to 300 m.

Cod vocalization detection and temporal–spectral characterization

Each beam-time series was converted to a beamformed spectrogram by short-time Fourier transform (sampling frequency = 8000 Hz, frame = 2048 samples, overlap = 3/4, Hann window). For the pair of B&K hydrophones, the raw pressure–time series data were converted to spectrograms by

Downloaded from https://academic.oup.com/icesjms/advance-article/doi/10.1093/icesjms/fsad104/7218794 by guest on 09 August 2023

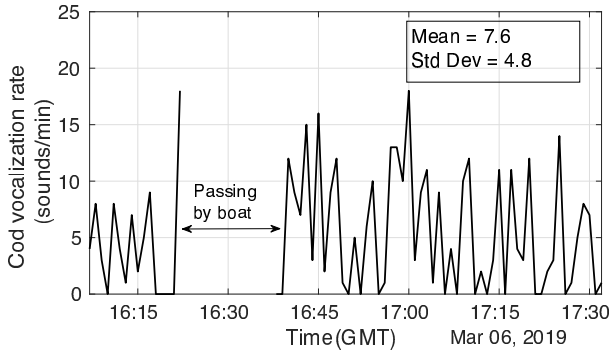

Figure 6. Vocalization rate of detected cod sounds in Austevoll, by B&K hydrophone on 6 March 2019. Between 16:23 and 16:37 GMT, cod vocalizations could not be detected because of the significantly high noise level caused by a passing boat.

short-time Fourier transform. The spectrogram images from both the B&K hydrophones and the hydrophone array were overwhelmed with long-duration tonal sounds at discrete frequencies radiated from RV Hans Brattstrøm due to close proximity of the ship's engines to the sensors (Figure 2a). The cod vocalizations received on the hydrophones were comparatively impulsive with short time durations of <0.3 s. To distinguish cod vocalizations from own ship-radiated tonal sounds, we calculated the horizontal time derivative of spectrogram intensity images (Oppenheim, 1997). This procedure significantly reduced the intensity of ship tonal signals in the resulting time-differenced spectrogram intensity output, thus enhancing the detection of impulsive cod grunt signals (Figure 2b). Significant signals present in time-differenced spectrogram intensity images, such as cod grunts, were automatically detected by first applying a pixel intensity threshold detector (Sezan, 1990; Huang *et al.*, 2017; Garcia *et al.*, 2018), followed by pixel clustering, and verified by visual inspection. Time-differenced spectrogram pixels with local values that are 12 dB above the background were grouped using a clustering algorithm according to a nearest-neighbour criterion that determines if the pixels can be grouped into one or more significant sound signals. Time–frequency bounding boxes for significant signals present in the time-differenced spectrogram intensity outputs were noted. The significant signals detected using this approach were predominantly fish-produced sounds in the frequency range from 10 Hz to 1 kHz. The other strong signals from non-fish sources in this frequency range were ship-generated transients, which were removed from the set of fish sounds analysed here by visual inspection.

These time–frequency bounding boxes were then applied to the original spectrogram intensity data to derive cod grunt signal features. For each signal, the frequency, time, and mean square pressure per Hz are first extracted from each pixel (i, j) that exceeds the detection threshold, $f(i, j)$, $t(i, j)$, and $W(i, j) = P^2(i, j)$. Next, the following features are calculated for each detected cod signal: (i) minimum frequency f_{min} (Hz), (ii) maximum frequency f_{max} (Hz), (iii) power amplitude weighted average frequency $\bar{f}_w$ (Hz), (iv) peak power frequency fp (Hz), (v) bandwidth BW (Hz), and (vi) duration of detected vocalization τ (s), which is the threshold exceedance signal duration.

$$\text{(i)}\ f_{min} = \min_{i,j} f(i, j),\ \forall i, j \tag{1}$$

$$\text{(ii)}\ f_{max} = \max_{i,j} f(i, j),\ \forall i, j \tag{2}$$

$$\text{(iii)}\ \bar{f}_w = \sum_{i,j} f(i, j)W(i, j) / \sum_{i,j} W(i, j) \tag{3}$$

$$\text{(iv)}\ W_m(k, l) = \max_{i,j} W(i, j),\ \forall i, j$$

$$f_p = f(i = k, j = l) \tag{4}$$

$$\text{(v)}\ BW = f_{max} - f_{min} \tag{5}$$

$$\text{(vi)}\ \tau = \max_{i,j} t(i, j) - \min_{i,j} t(i, j),\ \forall i, j \tag{6}$$

In addition, from the detected signal time series [examples shown in Figure 3(a) and (b)], the (vii) number of amplitude peaks occurring in each time series was also extracted.

Source level distribution estimation for cod vocalizations

The source level $L_s(r_0)$ of each cod vocalization in units of dB re 1 μPa at 1 m was estimated from its received pressure level $L_p(r)$ by accounting for propagation loss via (in the section "Material and methods" of the Kinsler *et al.*, 1999 International Organization for Standardization, 2017, with similar concepts in Urick, 1983; Kinsler *et al.*, 1999; Garcia *et al.*, 2018),

$$L_s(\mathbf{r}_0) = L_p(\mathbf{r}) + N_{PL}(|\ \mathbf{r} - \mathbf{r}_0\ |). \tag{7}$$

where $\mathbf{r}$ is the location of the coherent hydrophone array centre, $\mathbf{r}_0$ is the mean location of the cod fish aggregation, $N_{PL}(|\mathbf{r} - \mathbf{r}_0|)$ is the acoustic transmission loss in units of dB re 1 m from the estimated location of cod vocalization to the centre of the coherent hydrophone array, and $L_p(\mathbf{r})$ is the received cod mean-square sound pressure level in units of dB re 1 μPa. Here, $L_p(\mathbf{r}) = 10\log_{10}\frac{\overline{P^2(\mathbf{r})}}{P_o^2}$, where $\overline{P^2}$ is the mean-square sound pressure of the cod vocalization signal and P_o^2 is the reference mean-square sound pressure of 1 μPa^2. Time-domain signal of cod vocalization is bandpass filtered between upper f_U and lower f_L frequencies and beamformed to the azimuthal bearing of the received cod vocalizations, over a time window encompassing >90% of the total signal energy.

PoD regions for coastal cod vocalizations

The POAWRS PoD $P_D(r)$ for cod vocalizations, as a function of range r from the coherent hydrophone array, is modelled using the approach provided in Appendix 1 of Garcia *et al.*, (2018) and in the online supporting material of Wang *et al.* (2016a). The calculations are centred at cod vocalization peak frequency of 60 Hz received on the coherent hydrophone array after spatial beamforming. The experimentally determined coastal cod vocalization source level distribution L_s along with stochastically modelled (Andrews *et al.*, 2009) range- and depth-dependent transmission loss (Collins, 1993; Collins and Siegmann, 2019) intensities for the area is applied as inputs in the PoD calculations. We model the PoD regions at four distinct array locations in Austevoll, including both shallow inlet and deeper surrounding areas. The PoD modelling approach employed here for cod vocalizations with a receiver array had been previously developed and applied to estimate PoD regions for humpback whale vocalizations (Gong *et al.*, 2014; Wang *et al.*, 2016b) in the Gulf of Maine, and fin whale vocalizations in the Norwegian and Barents Seas (Garcia *et al.*,

Downloaded from https://academic.oup.com/icesjms/advance-article/doi/10.1093/icesjms/fsad104/7218794 by guest on 09 August 2023

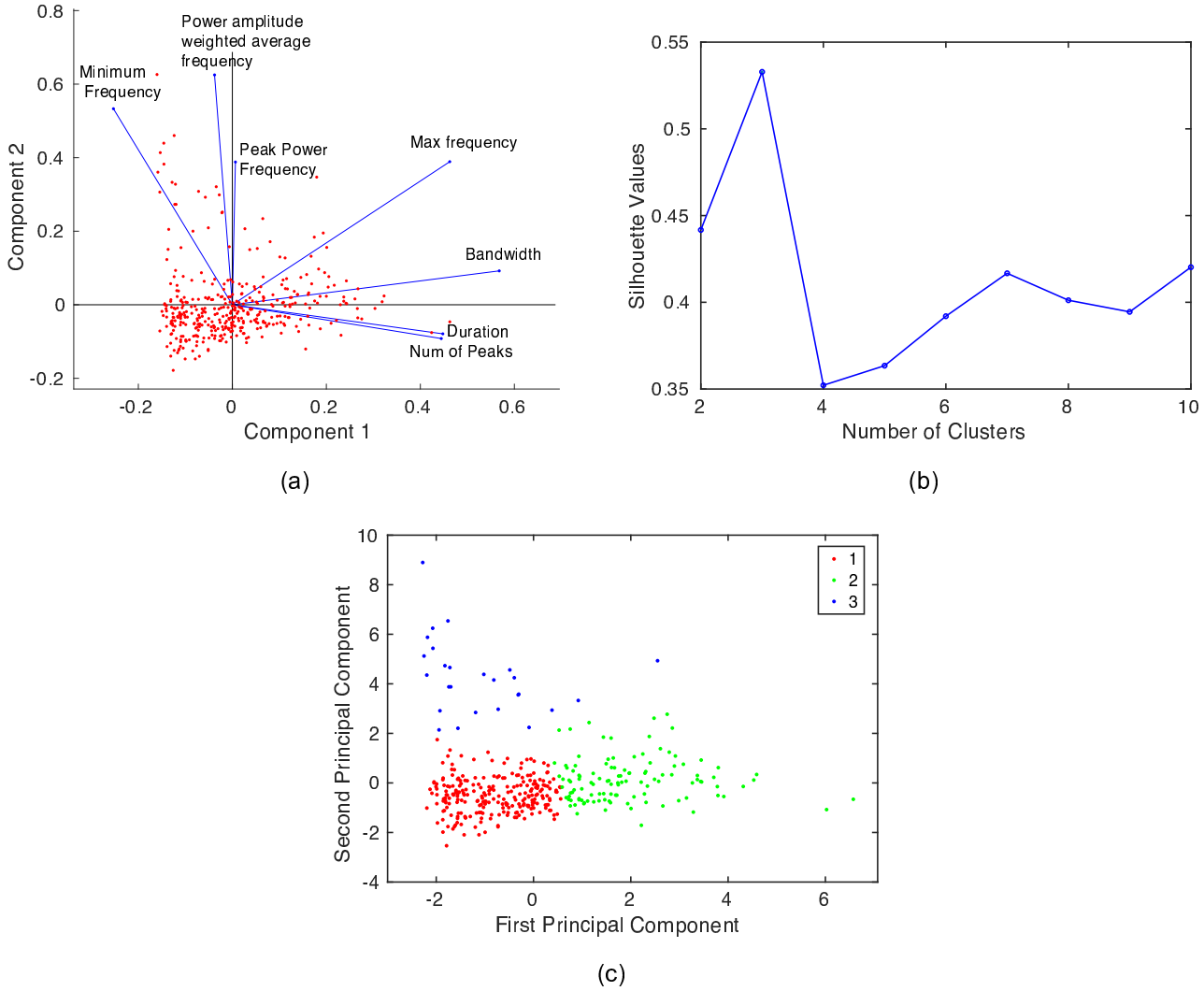

Figure 7. Automatic grouping of 388 shortlisted unlabelled detections measured on the B&K hydrophone on 6 March 2019. (a) Principal component coefficients for each feature variable and the principal component scores for each detected fish sound in a single plot. From this, we can derive that bandwidth and maximum frequency features contribute highest to component 1 and power amplitude weighted average mean frequency and minimum frequency contribute more to component 2. (b) Silhouette criterion values for each number of clusters tested. Highest silhouette value occurs at three clusters, suggesting that the optimal number of clusters is three. (c) Scatter plot showing the three different clusters on applying the k-means clustering algorithm.

2018) received on a larger coherent hydrophone array with multiple 64-element nested sub-apertures (see Supplementary Information section I and Supplementary Information Figure 1(b) of Wang *et al.* 2016b).

Results

First calculations of the statistical time–frequency feature parameters of observed cod vocalizations in Austevoll are presented for measurements based on a B&K hydrophone. For the eight-element hydrophone array, these parameters are presented separately in the stationary vertical and horizontal tow modes.

The cod sound time–frequency characteristics are presented separately based on sensor system and deployment mode because the received cod vocalization maximum and minimum frequencies, as well as bandwidth are dependent on the measurement scenario, depending on whether array gain is applicable or tow-induced flow noise is present. Next, the source level distribution for cod vocalizations estimated from vertically deployed hydrophone array measurements is provided. This distribution is then applied as an input to calculate the PoD regions for cod vocalizations with a hydrophone array as a receiver at multiple locations in Austevoll, including both shallow inlets and deeper surrounding slope waters. Finally, the spatial distribution of Norwegian coastal cod vocalization rates in Austevoll along the tow tracks of the hydrophone array is mapped.

Vertically deployed single B&K hydrophone

On 6 March 2019, the Norwegian coastal cod vocalizations were measured on a pair of B&K hydrophones deployed vertically between 17:00 and 18:32 GMT. The cod vocalizations consist of a series of individual transient sound pulses (Figure 3c), similar to observations of previous studies (Fudge and Rose, 2009; Hernandez *et al.*, 2013; Wilson *et al.*, 2014; Martijn, 2021). Based on automatic detection and verified by

Downloaded from https://academic.oup.com/icesjms/advance-article/doi/10.1093/icesjms/fsad104/7218794 by guest on 09 August 2023

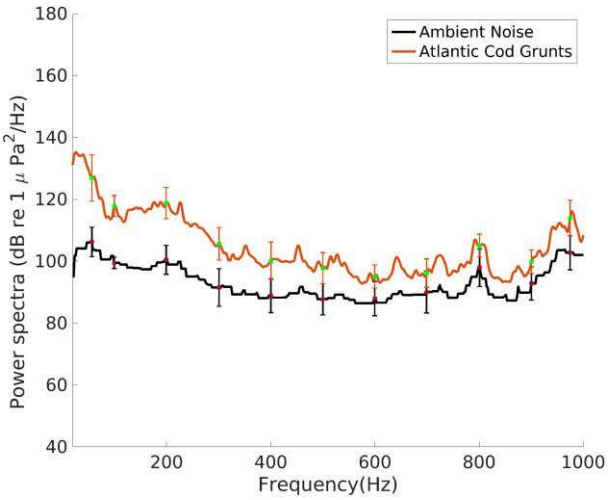

Figure 8. The mean spectra and standard deviation of detected cod vocalizations and ambient noise segments measured by a vertically deployed eight-element hydrophone array on 7 March 2019. The cod vocalization mean level stands clearly above the ambient noise mean level (>5.6 dB apart) at low frequencies till ~600 Hz, after which the error bars overlap.

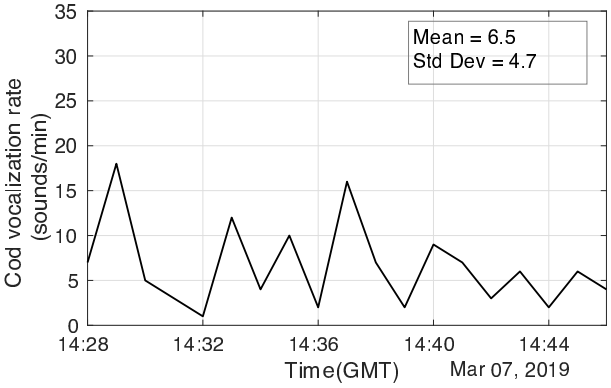

Figure 9. The vocalization rate of detected cod sound based on eight-element hydrophone array measurements while vertically deployed on 7 March 2019.

visual inspection, 388 detections were shortlisted to be cod vocalizations. Cod has been observed to produce multiple types of sounds, such as grunts, knocks, and a series of knocks, as observed by Midling *et al.* (2002). Example of cod grunt and knock signals received on a B&K hydrophone are shown in Figure 3(a) and (b), respectively. Classification of the 388 shortlisted signal detections was done both manually and automatically. A visual comparison of pulse shape and rate in signal time series, as well as signal duration was used in the manual classification of fish sounds. For automatic classification, all seven time–frequency features extracted from signal detections were employed.

Manual classification

The 388 shortlisted signals from the stationary B&K hydrophone were manually classified into four groups based on visual comparison of pulse rate and call duration to recorded sounds from net pens with spawning cod sampled from the same population. The four groups re "presumed cod grunt", "presumed cod knock", "unconfirmed", and "presumed false detections". After careful analysis perusing the time-series data and listening to the audio sound file of each shortlisted signal, 194 detections were considered to be presumed cod grunts, 119 presumed cod knocks, 45 unconfirmed, and the remaining 30 detections were found to be from some other source. The "unconfirmed" were later renamed as "cod unclassified" after statistical analysis and further examination of signal time series and sound playback. These findings are consistent with ANOVA (ANalysis Of VAriance) on frequency characteristics shown in Figure 4a and b and tabulated in Table 2. The one-way ANOVA (Figure 4a and b) shows there are significant differences in the minimum frequencies and power amplitude weighted frequencies of the three cod sound groups from the single non-cod sound "false detections" group. The small pairwise p-values of the multiple ANOVA analysis (in Table 2) between "false detections" with each of the other three cod sound groups suggest that the characteristics of minimum frequency and power amplitude weighted frequency for the "presumed false" detection category are significantly different from those of the presumed "cod grunt", "cod knock", and "cod unclassified" detection categories. These two characteristics are highly similar for the detections in the three cod sound categories based on their large pairwise ANOVA probabilities (p-values). Since knocks were observed in association with grunts (Figure 5), and given the large ANOVA p-values for the two frequency characteristics analysed, we assumed them to be from the same source type, the cod fish. The "cod unclassified" sounds are vocalizations that could not be clearly distinguished as grunts or knocks. These were sounds that could be classified as grunts, but had fewer than three clear consecutive pulses, which made it impossible to quantify pulse rate. The ANOVA analysis indicates the "cod unclassified" sound minimum frequency and power amplitude weighted frequency characteristics are highly similar to those for the "cod knock" sound.

Occasionally, we also observed grunt pulses that sounded reverberant, probably as a result of interference due to reflections off our ship hull or the sea surface. Analysis of these reverberant cod sounds is provided in the Appendix. The time–frequency parameters calculated from signal detections on one of the two B&K hydrophones are provided in Table 3 separately for each of the four groups.

Based on the B&K hydrophone measurement, the broadband frequency of cod grunts range from 21 ± 15 Hz (minimum frequency) to 119 ± 36 Hz (maximum frequency), with a mean peak power frequency ~69 ± 32 Hz. The average time duration of the cod grunts is found to be 0.3 ± 0.18 s. Knocks produced by coastal cod are in a similar frequency range except for the shorter time duration, 0.22±0.16 s. The mean rate of all vocalizations measured on a single B&K hydrophone is found to be ~8 ± 5 sounds min^{-1}. Figure 6 shows the variation of vocalization rates measured between 17:07 and 18:32 GMT. Between 16:23 and 16:37 GMT, cod sounds could not be detected because of the significantly high noise level caused by a passing boat.

Automatic classification

The previously defined seven features extracted from each detected signal, which are (i) minimum frequency (Hz), (ii) maximum frequency (Hz), (iii) power amplitude weighted average frequency (Hz), (iv) peak power frequency (Hz), (v) bandwidth (Hz), (vi) duration of detected vocalization, and (vii) number of peaks, are applied for automatic grouping of

Downloaded from https://academic.oup.com/icesjms/advance-article/doi/10.1093/icesjms/fsad104/7218794 by guest on 09 August 2023

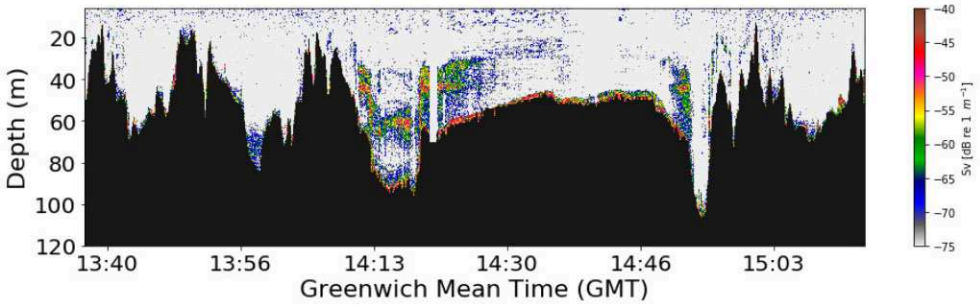

Figure 10. Echograms (38 kHz Sv vs. depth and time) showing the volume back-scattering strength (Sv [dB re 1 m^{-1}]) of individual echoes of fish (likely to be cod) in the Austevoll region. During the time interval from 14:28 to 14:46 P.M. of 7 March 2019, both the eight-element hydrophone array and B&K hydrophone pair were simultaneously acquiring data in vertical deployment mode.

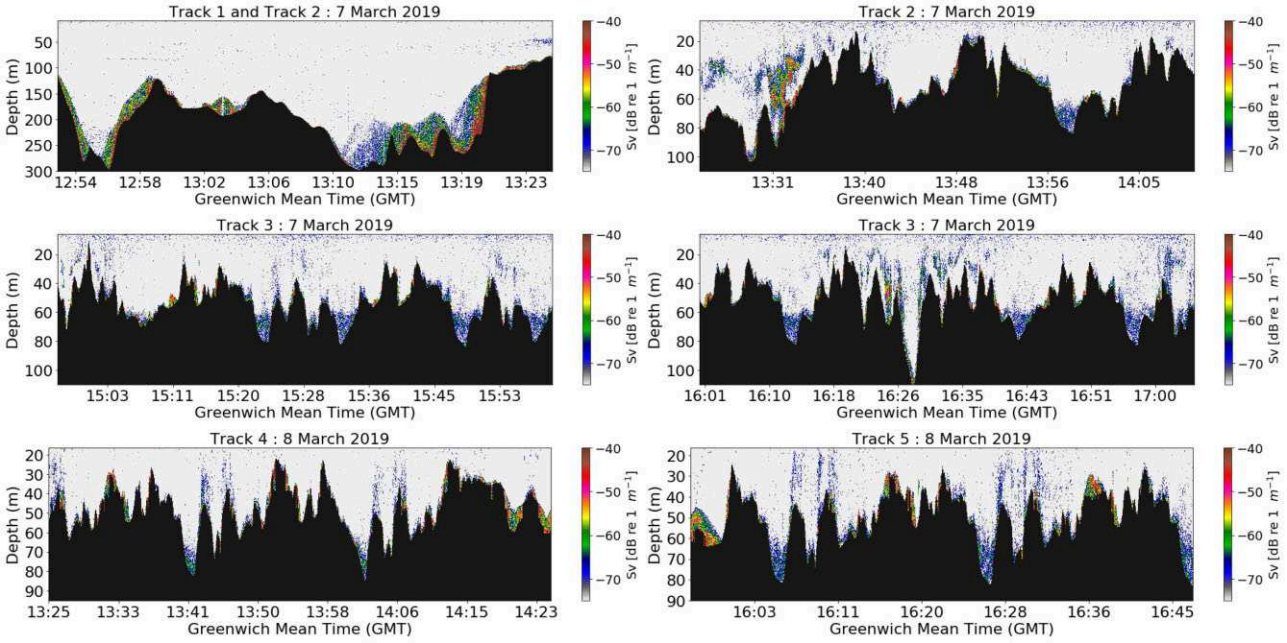

Figure 11. Echograms (38 kHz Sv vs. depth and time) showing the volume back-scattering strength (Sv [dB re m^{-1}]) of individual echoes of presumed coastal cod in the Austevoll region along the tow tracks of the eight-element hydrophone array on 7–8 March 2019.

sounds via cluster analysis. First, the extracted features are normalized and re-scaled into standardized form with a zero mean and unity standard deviation. Feature scaling is necessary to ensure that all the features receive the same weightage or importance in the clustering analysis. The vector of normalized features from each detection that constitutes a set of potentially correlated variables is then transformed into a set of linearly uncorrelated variables using principal component analysis (PCA). The PCA technique is often used for feature selection and dimension reduction. The dominant components are next used to classify the different groups of signal detections via k-means clustering method. Figure 7(a) shows the bandwidth and max frequency are the most contributing features for the first principal component, whereas mean frequency and minimum frequency are the most contributing features for the second principal component. The k-means clustering algorithm, a recursive approach that determines distinct clusters by minimizing the distance of each feature vector from the cluster centre, is used here. The optimal number of clusters is determined by evaluating the silhouette criterion (Rousseeuw, 1987) values. From Figure 7(b), it was found that the highest silhouette value occurs at three clusters, indicating the optimal number of clusters. Figure 7(c) shows three distinct clusters using the first two principal components with 246 detections in cluster 1115 detections in cluster 2, and 27 detections in cluster 3. The time–frequency characteristics of each cluster type are quantified in Table 4. Cluster 3's minimum frequency, power amplitude weighted average frequency, and peak frequency are found to be distinct from the other clusters. This suggests that cluster 3 contains false detections, that is, non-cod sounds. Table 5 shows the distribution of manually labelled fish sounds in different clusters. Manually labelled grunts account for around 66% of cluster 2 detections. Cluster 1 contains a mix of manually labelled grunts (45%) and knocks (38%). Given the clear difference in the number of peaks between clusters 1 and 2 (mean 2.3 vs.

Downloaded from https://academic.oup.com/icesjms/advance-article/doi/10.1093/icesjms/fsad104/7218794 by guest on 09 August 2023

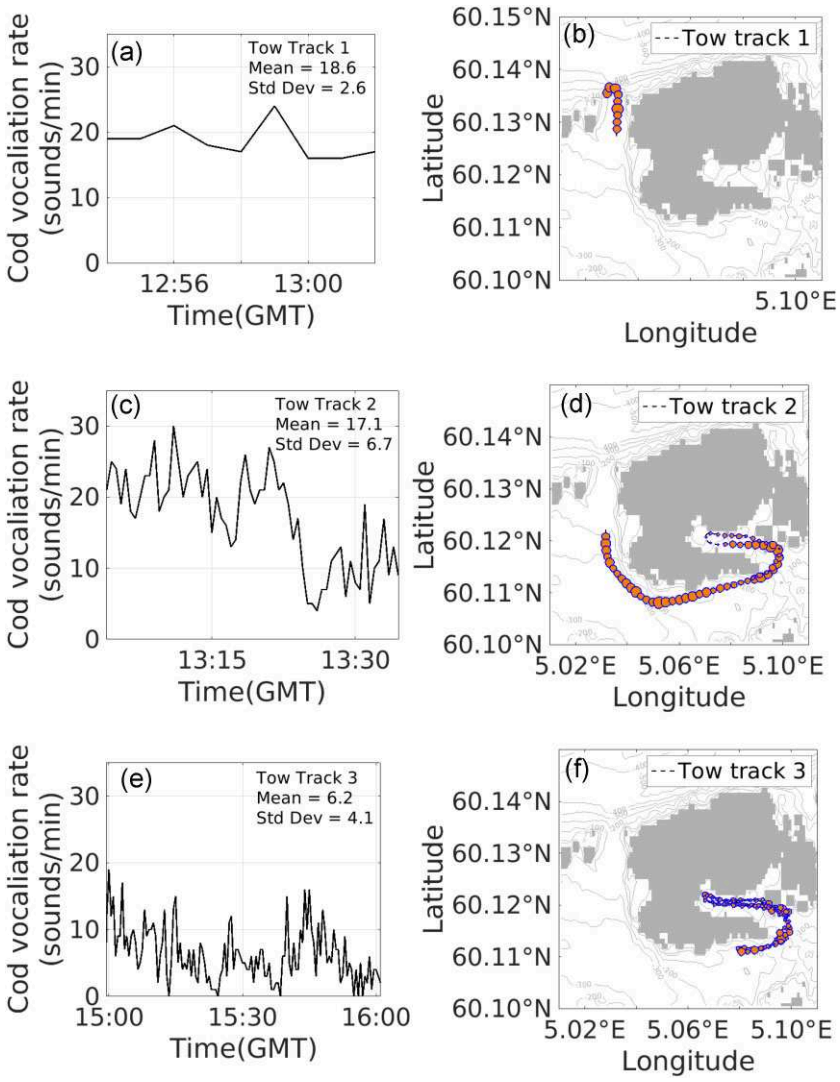

Figure 12. Rates of detected coastal cod vocalizations measured by hydrophone array while horizontally towed (along tracks 1, 2, and 3) in Austevoll on 7 March 2019. Size of the circle is proportional to cod vocalization rate. Note that vocalizations probably emerge from cod fish located within an ∼1 km radius of the array (see Figure 15a and d) for the hydrophone array in deeper slope areas and within a 0.25 km radius of the array in shallow inlet areas.

7.75), it is clear that cluster 2 is important for grunts, whereas cluster 1 is likely a mixture of knocks and shorter-duration grunts.

Both the manual and automatic classification indicate that over 93% of the shortlisted detections are consistent with cod sounds and that the non-cod (false) sounds comprise <7% of the shortlisted detections (see confusion matrix, Table 5). For the remaining analysis, we do not further sub-classify the shortlisted signals after automatic detection and visual inspection, since further sub-classification can be laborious and the non-cod sounds are expected to be <7% of the shortlisted detections. We refer to the shortlisted detections as cod detections in the rest of the paper.

Vertically deployed hydrophone array

The eight-element hydrophone array was deployed vertically on 7 and 8 March 2019 in Austevoll. The raw pressure–time series data from eight hydrophones is beamformed to enhance the signal-to-noise ratio (SNR) of detected cod sounds by rejecting noise outside of the signal beam. We can observe from Figure 2 that beamforming helps to enhance higher frequency components making cod vocalization energy detectable up to 600 Hz (see Figure 8) due to higher array gain at those frequencies when compared to single hydrophone measurements. Time–frequency parameters calculated from cod vocalization detections of the vertically deployed hydrophone array are tabulated in Table 6. The minimum frequency and power amplitude weighted frequency of detections in the vertically deployed array measurements are in good agreement with those from cod sound detections with the B&K hydrophone. The maximum frequency and bandwidth from analysis of vertical hydrophone array measurements are roughly double those calculated from B&K hydrophone measurements due to a higher SNR enhancement gain at upper end of the cod sound spectrum from beamforming. Figure 9 shows the cod vocalization rates measured by the hydrophone array when deployed vertically on 7 March 2019.

Echosounder measurements reveal the depth distribution and abundance of fish before, during, and after the vertical hydrophone array deployment. As shown in Figure 10, a fish shoal, likely to be cod, is present in the immediate vicinity at ∼30–60 m water depth.

Downloaded from https://academic.oup.com/icesjms/advance-article/doi/10.1093/icesjms/fsad104/7218794 by guest on 09 August 2023

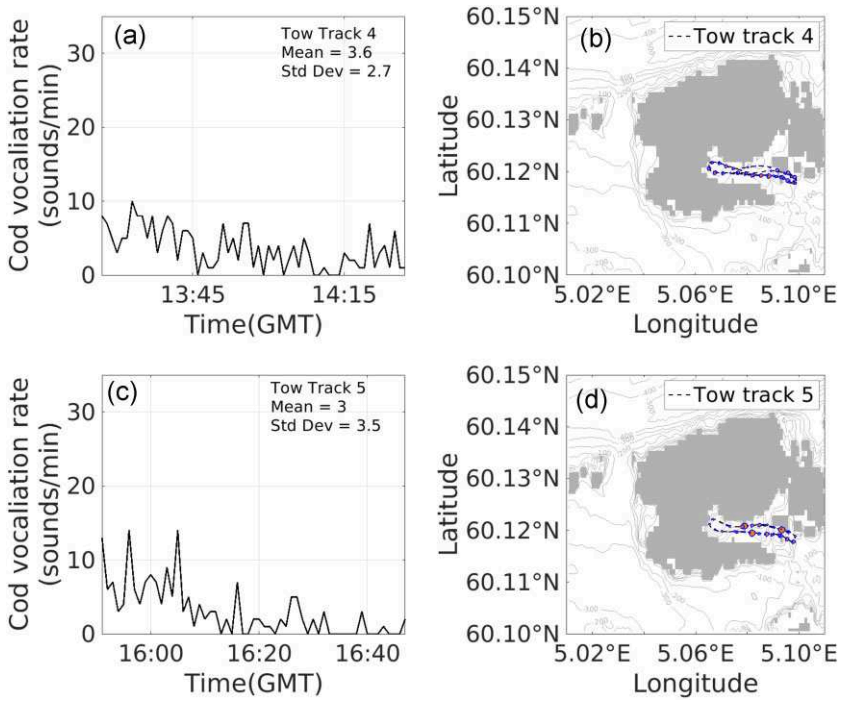

Figure 13. Vocalization rates as a function of time (a, c, and e) and space (b, d, and f) of detected coastal cod measured by a hydrophone array while horizontally towed (along tracks 4 and 5) in the Austevoll region on 8 March 2019. Size of the circle is proportional to cod vocalization rate. Note that vocalizations probably emerge from cod fish located within a roughly 1 km radius of the array (see Figure 15a and d) for the hydrophone array in deeper slope areas and within a 0.25 km radius of the array in shallow inlet areas.

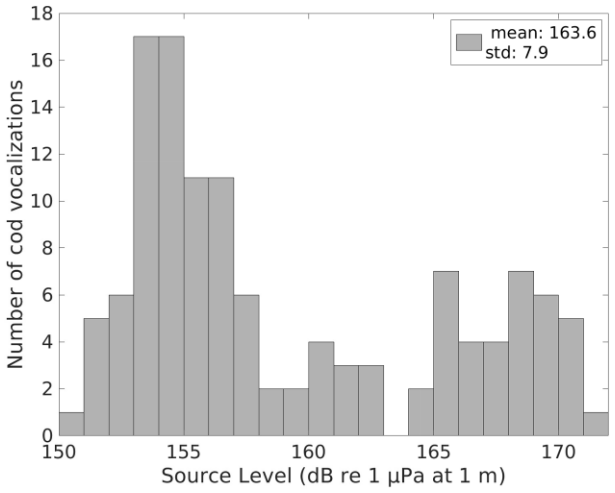

Figure 14. Histogram of back-projected source level estimates of 124 detections of Austevoll cod vocalizations. The estimated back-projected source levels range from 150 to 172 dB re 1 μPa at 1 m with a mean and standard deviation of 163.5 ± 7.9 dB re 1 μPa at 1 m.

Horizontally towed hydrophone array

Data acquired by the horizontally towed eight-element hydrophone array are divided into five distinct segments (or tracks) over 2 d. The time frequency characteristics of detected cod vocalizations based on analysis of towed hydrophone array data are listed in Table 7. The minimum detectable frequency has increased from 22 Hz in stationary vertical mode to roughly 36 Hz in horizontal tow mode likely due to increased flow noise on the array at low frequencies from towing. The array has a simple design consisting of a tow cable connected directly to an eight-element hydrophone acoustic aperture, with no vibration isolation module in between to dampen the flow noise.

Cod sound detection rates were higher along tracks 1 and 2 compared to the other tracks. Furthermore, larger measured cod sound rates are associated with a higher maximum frequency parameter of 300 ± 100 Hz for track 1 and 238 ± 94 Hz for track 2, whereas the maximum frequency parameter obtained from tracks 3, 4, and 5 was ~186 ± 33 Hz. The mean durations of the detected cod vocalizations are approximately equivalent over the five tracks (~0.3 s). The simultaneously acquired echo-sounder output for each track is shown in Figure 11, confirming the presence of fish in the vicinity. Based on the target strength, depth distribution, and knowledge of species abundance in the area from local fishermen, these are most likely cod.

Measured cod vocalization rates in units of sounds/min were calculated from the towed hydrophone array measurements along its five tracks and mapped in geographic space. On 7 March 2019, the hydrophone was towed at different times of the day with measurements grouped into three distinct tracks (Figure 12). Mean detected cod vocalization rate along track 1 in the slope water region where water depths are deeper than 100 m is observed to be 18 ± 3 sounds min^{-1}. The detected cod vocalization rate of track 2, which goes from deeper slope water into shallow inlet water, varied from roughly 25 calls min^{-1} initially to 8 per minute calls in the inlet area, with overall mean of 17 ± 7 sounds min^{-1}. Coastal cod vocalization rate for track 3 varied from 18 to 0 sounds min^{-1} with a mean of 6.2 ± 4. On 8 March 2019, two tow tracks of the horizontal hydrophone array are available (Figure 13).

Downloaded from https://academic.oup.com/icesjms/advance-article/doi/10.1093/icesjms/fsad104/7218794 by guest on 09 August 2023

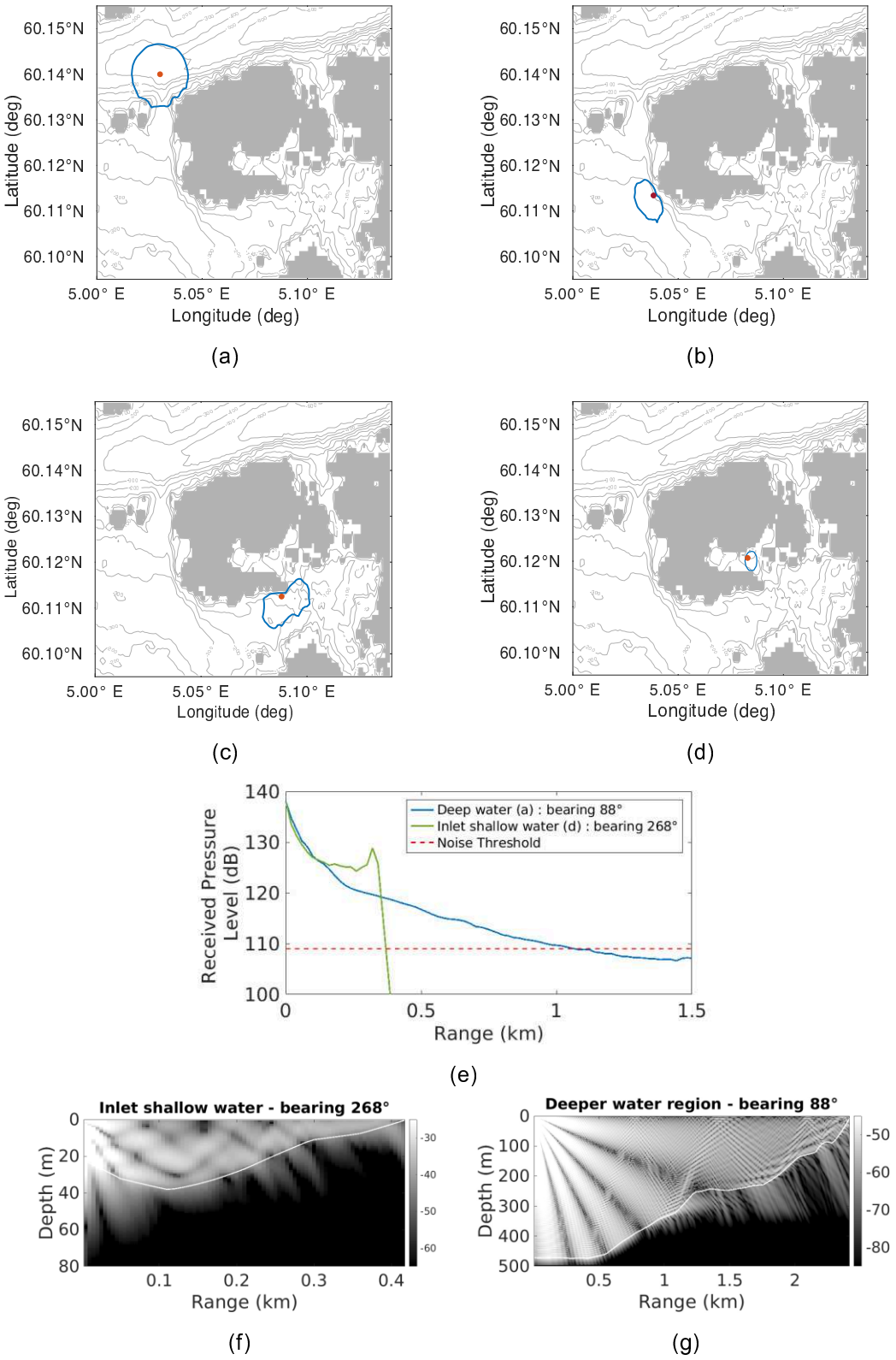

Figure 15. The PoD region for coastal cod vocalization centred at 60 Hz received on eight-element hydrophone array at various locations, both deeper slopes and shallow inlet areas, in Austevoll. The blue solid contours in (a)–(d) provide the 50% PoD areas after beamforming. Examples of received pressure level as a function of range calculated by a calibrated parabolic equation-based range-dependent acoustic propagation model (Collins, 1993; Collins and Siegmann, 2019) along two propagation paths with the following directions: 88° from true north [deeper channel area in (a)] and 268° from true north [shallow inlet area in (d)] are shown in (e). The transmission losses for the corresponding directions are plotted in (f–g), as a function of propagation range and depth.

Downloaded from https://academic.oup.com/icesjms/advance-article/doi/10.1093/icesjms/fsad104/7218794 by guest on 09 August 2023

Tracks 4 and 5 are in the shallow inlet area with small detected call rates and a mean of ~3 calls min^{-1} for both tracks.

Many factors such as water depth, season, diel cycle, lunar cycle (Thorsteinsson *et al.*, 2012; Grabowski *et al.*, 2015; Zemeckis *et al.*, 2019; Caiger *et al.*, 2020), and water temperature affect the spawning activity of coastal cod. Here, the detected coastal cod grunt rates were highest in the deeper slope water areas, and lowest in the shallow inlet areas. The new moon started after 6 March 2019 at 17:00, but our observation time period was not wide or long enough to assess the full effect of the lunar cycle.

Source level distribution and PoD regions for cod vocalizations

The received pressure level (L_p) of the majority of cod vocalization detections measured by the coherent hydrophone array when vertically deployed is found to be in the range of 120–140 dB re 1 μPa. The transmission loss is calculated by averaging cod depths from 20 to 60 m with a mean of 40 m (the one-way transmission loss for this mean depth is 32 dB re 1 m), as can be deduced from Figure 10. The corresponding source level distribution is derived from the received pressure levels of the cod vocalization detections after correcting for transmission losses, assumed to be geometrical spherical spreading loss at these short ranges. The estimated source levels of 128 detected cod vocalization signals range from 150 to 172 dB re 1 μPa at 1 m (Figure 14). The mean and standard deviation for cod vocalization source level distribution are found to be 163.5 ± 7.9 dB re 1 μPa at 1 m.

The estimated source level distribution of cod vocalizations is applied as an input to calculate the PoD region for the coherent hydrophone array as a receiver. The array gain (Urick, 1983) values from Table 8 for cod vocalizations were used in the PoD calculations to account for SNR enhancement after beamforming with the eight-element hydrophone array. The 50% PoD region for cod detection with the hydrophone array at four distinct locations is plotted in Figure 15(a)–(d). The water depth for the array location shown in Figure 15(a) is around 300 m, while the water depths for the array locations shown in Figure 15(b), (c), and (d) are ~150–200, 100, and 30 m, respectively.

The PoD areas for cod vocalization detection are quite small, extending over an area of roughly 2 km in diameter for the deeper slope water site and about 0.7 km in diameter at the shallow inlet. These PoD areas are significantly impacted by large bathymetric variations over the region and especially in shoreward directions and the shallow-water inlet, where there is substantial penetration and absorption of sound into the sea bottom (Figure 15e–g).

Discussion

In this study, cod vocalizations in a shallow-water inlet and deeper surrounding slope areas of a coastal bay at Austevoll, western Norway have been studied and quantified in terms of time–frequency characteristics, source level distribution, and spatial dependencies from measurements with an eight-element towable hydrophone array. Here we discuss and compare our results with those in the published literature, including implications for future fisheries research.

In terms of time–frequency characteristics, previous studies provide various frequency ranges for coastal cod vocalizations (typically below 1000 Hz). Stanley *et al.* (2017) showed that the frequency range for Atlantic cod vocalizations is 30–500 Hz, recorded using Marine Autonomous Recording Units (MARU) sampled at a rate of 2 kHz. Similarly, Hernandez *et al.* (2013) analysed US Atlantic cod vocalizations using MARU recordings at a sampling rate of 5 kHz and found their frequency range to lie between 20 and 250 Hz. It was shown that ambient sound levels in the Norwegian Lofoten coast were increased by 7–18 dB between 50 and 500 Hz during the cod spawning period, presumably due to cod vocalizations (Nordeide and Kjellsby, 1999). In our study, we were able to detect coastal cod vocalizations up to 200 Hz with a single B&K hydrophone with 8 kHz sampling rate. Much higher maximum frequencies of up to 600 Hz were detectable for cod vocalizations after coherent beamforming with the eight-element hydrophone array. This hydrophone array is designed to provide unaliased beamforming for time harmonic signals at frequencies up to 1 kHz, and provides better SNR enhancement for broadband signals, almost 9 dB, near the hydrophone array design frequency of 1 kHz. However, at the cod sound peak energy frequency of roughly 60 Hz, the array gain for the eight-element hydrophone array is negligibly small with the PoD area nearly equivalent to that for a single hydrophone. Larger hydrophone arrays with a greater number of elements would be needed to increase array gain and hence PoD area at the cod sound peak frequency of 60 Hz (see Table 8).

Previous studies (Brawn, 1961; Nordeide and Kjellsby, 1999; Rowe and Hutchings, 2006) observed that sound production occurs most frequently during the spawning period, particularly after the onset of darkness. Caiger *et al.* (2020) investigated spatio-temporal trends of cod vocalizing over 10 consecutive winter spawning seasons using multiple fixed-station passive acoustic recorders to sample across Massachusetts Bay. It was indicated that the highest grunting activity was near sunset and at night. In contrast, Hernandez *et al.* (2013) showed that cod grunts in Massachusetts Bay were most prevalent during daylight hours as opposed to twilight and nighttime hours. In the current experiment, most of the recordings were made during daylight hours between noon to dusk. The cod grunts rates varied and included both high and low daytime levels depending on the location. On average, higher grunt rates were observed in deeper surrounding slope water than shallow inlet areas. This result may also be due to better propagation conditions and a larger PoD area for cod grunt detection in slope areas than in shallow inlet areas. Longer observation time periods covering multiple diurnal cycles in each of the areas investigated, both shallow inlet and deeper slope areas, would be needed to ascertain potential day-to-night variations of cod grunt rates and their dependence on location. An advantage of the hydrophone array is that it is mobile and can readily traverse several distinct sites over multiple diurnal cycles to make the necessary measurements, which is planned for future studies.

Spawning is an essential part of stock recruitment and understanding spawning behaviour and how disturbances such as intense sound sources affect this behaviour is important (de Jong *et al.*, 2020). By using a combination of acoustic telemetry and archival data storage tags, Siceloff and Howell (2013) demonstrated that Atlantic cod in the western Gulf of Maine aggregate around fine-scale bathymetric features on the spawning ground, utilize relatively small areas during spawning, are highly mobile within those areas, and tend to move as a group. In contrast to most studies, Sund (1935) and

Downloaded from https://academic.oup.com/icesjms/advance-article/doi/10.1093/icesjms/fsad104/7218794 by guest on 09 August 2023

Table 2. Multiple comparisons between detected cod sounds and non-cod sounds for minimum frequency and power amplitude-weighted frequency characteristics.

Group A	Group B	*p* value for power amplitude Weighted frequency	*p* value for Minimum frequency
"Grunts"	"Knocks"	0.43	0.84
"Grunts"	"Unclassified"	0.14	0.29
"Grunts"	"False"	6.01e-08	6.15e-09
"Knocks"	"Unclassified"	0.74	0.69
"Knocks"	"False"	1.93e-05	1.98e-07
"Unclassified"	"False"	0.0061	0.00045

The first two columns show the pair of groups that are compared. The third and fourth columns show the *p*-value for a hypothesis that the true difference of means for the corresponding groups is equal to zero.

Table 3. Time–frequency characteristics of "manually labelled" 388 detections received on a B&K hydrophone on 6 March 2019 in the Austevoll region.

Time–frequency characteristics	Cod grunts	Cod knocks	Cod unclassified	False
Min frequency (Hz)	21 ± 15	25 ± 19	28 ± 21	42 ± 32
Max frequency (Hz)	119 ± 36	115 ± 31	106 ± 34	136 ± 40
Power amplitude weighted average frequency (Hz)	62 ± 14	63 ± 18	67 ± 21	83 ± 26
Peak power frequency (Hz)	69 ± 32	66 ± 30	66 ± 34	81 ± 38
Bandwidth (Hz)	98 ±39	90 ± 32	78 ± 35	94 ± 43
Duration (s)	0.3 ± 0.18	0.22 ± 0.16	0.26 ± 0.18	0.35 ± 0.24

The detections are divided into four sub-classes—cod grunts (194), cod knocks (119), unclassified (45), and presumed false detections (30).

Table 4. Time–frequency characteristics of 388 detections received on a B&K hydrophone using "clustering analysis". The detections are divided into three call types based on k-means clustering.

Time–frequency characteristics	Cluster 1 (246)	Cluster 2 (115)	Cluster 3 (27)
Min frequency (Hz)	22 ± 9	17 ± 5	84 ± 28
Max frequency (Hz)	97 ± 19	152 ± 30	157 ± 23
Power amplitude weighted average frequency (Hz)	59.39 ± 10	64 ± 14	112 ± 23
Peak power frequency (Hz)	64 ± 29	70 ± 32	108 ± 38
Bandwidth (Hz)	75 ± 22	135 ± 30	73 ± 30
Duration (s)	0.21 ± 0.11	0.42 ± 0.21	0.17 ± 0.12
Number of peaks	2.3 ± 2	7.75 ± 6.1	1.8 ± 3.1

Table 5. Distribution of manually labelled grunts, knocks, unclassified cod, and false detections in each cluster analysis grouping is shown.

Manually labelled class	Cluster 1 (246)	Cluster 2 (115)	Cluster 3 (27)
Grunts (194)	45.1% (111)	66.1%(76)	26% (7)
Knocks (119)	38.2% (94)	16.5% (19)	22.2% (6)
Unclassified (45)	13% (32)	7.8% (9)	14.8% (4)
False (30)	3.7% (9)	9.6% (11)	37% (10)

Table 6. Time–frequency characteristics of 124 detected cod vocalizations based on on eight-element hydrophone array measurements when vertically deployed on 7 March 2019.

Time–frequency Characteristics	Cod vocalizations on hydrophone array (vertically deployed)
Min freq (Hz)	22.5 ± 13.6
Max freq (Hz)	199.1 ± 170.7
Power amplitude weighted average freq (Hz)	53.8 ± 31.4
Peak power freq (Hz)	41.8 ± 29.0
Bandwidth (Hz)	176.5 ± 169.0
Duration (s)	0.4 ± 0.3

Downloaded from https://academic.oup.com/icesjms/advance-article/doi/10.1093/icesjms/fsad104/7218794 by guest on 09 August 2023

Table 7. Time–frequency characteristics of detected cod vocalizations based on horizontally towed eight-element hydrophone array measurements of 7–8 March 2019.

Time–frequency characteristics	Track 1 (167)	Track 2 (1061)	Track 3 (779)	Track 4 (217)	Track 5 (173)
Min freq (Hz)	33.8 ± 19.8	38.6 ± 27.4	35.2 ± 13.6	38.6 ± 16.6	39.8 ± 19.2
Max freq (Hz)	308.5 ± 101.6	237.6 ± 94	187.4 ± 27.4	186.3 ± 30.7	183.6 ± 39.8
Power amplitude weighted average freq (Hz)	54.3 ± 44	65.5 ± 57.6	57.7 ± 28.2	62.4 ± 27	66 ± 35.3
Peak power freq (Hz)	40 ± 31.5	53 ± 60	45.3 ± 28	50.8 ± 26.4	50.6 ± 32.2
Bandwidth (Hz)	274.6 ± 98	199 ± 89.2	152.2 ± 28	147.6 ± 33.3	143.7 ± 37.7
Duration (s)	0.3 ± 0.14	0.31 ± 0.15	0.32 ± 0.16	0.27 ± 0.13	0.3 ± 0.18

Table 8. The eight-element array parameters at 60 Hz with array element spacing of 0.75 m are used in modelling the PoD areas for cod vocalizations in the Norwegian Sea.

$\bar{f}(Hz)$	Number of array elements	Array element spacing (m)	AG (dB)
60	8	0.75	0.27
60	64	0.75	4.02
60	64	1.5	7.02
500	8	0.75	6.19
500	64	0.75	13.22
500	64	1.5	16.23

They are the power amplitude-weighted average frequency, $\bar{f}$ (Hz), and coherent beamforming gain of the passive receiver array, AG. Note that higher array gains for fish sound detection can be achievable with a larger array with a greater number of elements, and they are listed here for comparison.

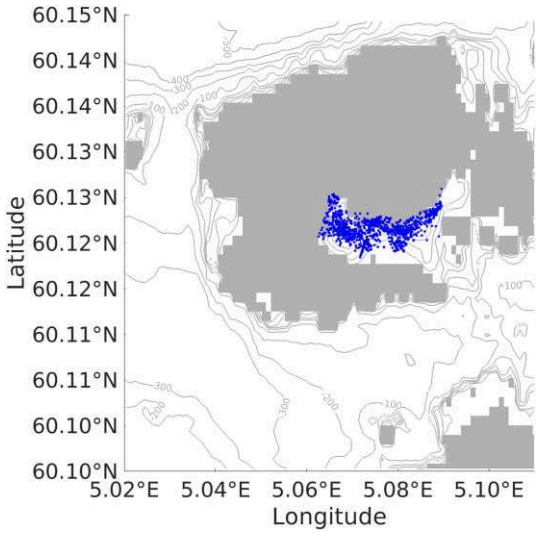

Figure 16. GPS locations of tagged coastal cod fish in the Austevoll region between 6 and 9 March 2019 are shown in blue.

Ingvaldsen *et al.* (2017) detected Atlantic cod in mid-water over deep-water basins using echosounding. Acoustic registrations of fish from the northern Fram Strait portion revealed that cod were present from ∼150 to >600 m above the continental slope, as well as in a 300–500 m deep layer off the slope (Ingvaldsen *et al.*, 2017).

Passive towed hydrophones consisting of eight sensors have been previously used by Holt (2008) to determine the spawning sites of red drum fish. It was indicated that the spawning activity of red drum is widespread and not concentrated at inlets. Similarly, in our survey, we observed roughly six times higher grunt rates (Figure 12) for cod in deeper slope water when compared to shallow inlet areas. To take into account the differences in PoD for cod sounds at these two locations with the hydrophone array, we divide the mean cod sound detection rate with the PoD area to derive a spatial vocalization detection rate in units of vocalizations/(km^2 min). The cod sound mean spatial vocalization detection rate for deeper water from Figure 15(a) is 10.75 ± 1.5 vocalizations/(km^2 min) and for shallow inlet area [in Figure 15(d) is 26 ± 30 vocalizations/(km^2 min)]. These values are now closer with a factor of 2.6 difference in favour of the shallow inlet area, as opposed to the previous factor of 6 difference in favour of the deeper site when the PoD areas were not taken into account. This analysis indicates that further studies and measurements may be needed to ascertain that (i) the cod call rates are truly higher in the deeper slope water, perhaps due to more cod abundance, or (ii) the detected call rates are higher due to the larger PoD area there compared to the shallow inlet area.

Figure 16 shows the locations of tagged cod in the shallow inlet part of the study area between 6 and 8 March 2019. We can observe that the tagged fish (26 different fish) are concentrated at inlets. However, since only this bay has been monitored, there is no information about fish movement and concentrations in the deeper areas.

The use of a large-aperture (>100 hydrophones) towable hydrophone array can be a great asset for studying the temporo-spatial distribution of cod via passive acoustics in future studies. A large-aperture densely populated array with many more elements such as the newly developed 160-element Northeastern University coherent hydrophone array (Schinault *et al.*, 2022; Radermacher *et al.*, 2022; Mohebbi-Kalkhoran *et al.*, 2022) with roughly 194 m acoustic aperture length, which provides a much higher array beamforming gain, larger SNR enhancement, and hence has a larger instantaneous PoD region for detecting cod vocalizations, would be advantageous for future monitoring of cod sounds. The hydrophone array can be towed from a mobile platform to provide monitoring of many different regions of interest during an experiment.

It should be noted that a limitation of passive acoustics is that detection requires fish to be vocally active, and also requires the sensor to be in the vicinity of the fish, especially so for single hydrophone measurements that have no array gain for signal enhancement. Since it may be mainly the male cod fish that produces sound (Rowe and Hutchings, 2006), as well as the fact that males and females are potentially distributed differently during spawning (Meager *et al.*, 2009; Dean *et al.*, 2014), the passive acoustic method should be used in combination with other methods, such as active acoustic echosounding, tagging, or fishing, for a more complete picture of fish distribution and behaviour.

Downloaded from https://academic.oup.com/icesjms/advance-article/doi/10.1093/icesjms/fsad104/7218794 by guest on 09 August 2023

Conclusion

Cod vocalizations have been detected and characterized based on observations from 6 to 8 March 2019 in the Austevoll region of the Norwegian coast using an eight-element towable coherent hydrophone array. Coherent beamforming combined with temporal differencing of spectrograms of the hydrophone array data is shown to significantly enhance the cod vocalization SNR in the presence of strong long-duration tonal sounds of the research vessel. The time–frequency characteristics of these vocalizations and their occurrence rate time series have been quantified from the deeper slope region to the shallow inlet region. The received sound pressure levels of cod vocalizations are quantified and applied to estimate the source level distribution. The detected coastal cod vocalization rate is mapped spatially along the tow tracks of the hydrophone array. The PoD areas have been estimated for cod vocalization detection with a hydrophone array receiver at multiple observation locations encompassing shallow inlet and deeper slope waters.

It should be noted that this study did not intend to survey the entire spawning habitat, but rather to examine the methodology and possibility for mapping of spawning habitats. The results of the spatial distribution of coastal cod vocalizations suggest that vocalization activity is possibly widespread to deeper water and is not concentrated at known spawning grounds. It could also be that the cod regularly stray away from the spawning ground and vocalize during other activities. This level of spatial resolution could not typically be obtained using traditional scientific data collection approaches. The use of a towed coherent hydrophone array can be an efficient means to determine the full extent of cod spawning areas provided that the relationship between vocalizations and spawning behaviour and other behaviours is more accurately described in future studies. Passive monitoring in additional areas with the help of a towed hydrophone array can give a larger scale understanding of biological sound production in ocean ecosystems and provide long-term temporo-spatial information on the occurrence of spawning events. The information gathered in this study can serve as a valuable guide for future research and can help inform future fisheries management actions.

Competing interests

The authors declare no competing interests.

Author contributions

All authors were involved in experimental design and data collection. Acoustic instrumentation and data acquisition were developed or configured by M.E.S., S.M.P., and S.G.S., with inputs from N.O.H. and P.R. Acoustic data were analysed by S.G.S. with inputs from K.D.J., N.O.H, L.D.S., and P.R. Ultrasonic echosounding and tagging data were provided by N.O.H. The paper was written by S.G.S and edited by P.R. with inputs from K.D.J., N.O.H., and L.D.S.

Data availability

The data underlying this article will be shared on reasonable request to the corresponding author.

Funding

This research was supported by the US National Science Foundation with grant numbers OCE-1736749 and OCE-2219953, the US Office of Naval Research with grant numbers N00014-20-1-2026, N00014-20-1-2358, and N00014-23-1-2327, and the Norwegian Institute of Marine Research via the SpawnSeis project with NFR grant number 280367.

References

Andrews, M., Chen, T., and Ratilal, P. 2009. Empirical dependence of acoustic transmission scintillation statistics on bandwidth, frequency, and range in New Jersey continental shelf. The Journal of the Acoustical Society of America, 125: 111–124.

Brawn, V. M. 1961. Sound production by the cod (*Gadus callarias* L.). Behaviour, 18: 239–255.

Caiger, P. E., Dean, M. J., DeAngelis, A. I., Hatch, L. T., Rice, A. N., Stanley, J. A., Tholke, C. *et al.* 2020. A decade of monitoring Atlantic cod *Gadus morhua* spawning aggregations in Massachusetts Bay using passive acoustics. Marine Ecology Progress Series, 635: 89–103.

Collins, M. D. 1993. A split-step padé solution for the parabolic equation method. The Journal of the Acoustical Society of America, 93: 1736–1742.

Collins, M. D., and Siegmann, W. L. 2019. Parabolic Wave Equations with Applications. Springer, New York.

Cote, D., Moulton, S., Frampton, P., Scruton, D., and McKinley, R. 2004. Habitat use and early winter movements by juvenile Atlantic cod in a coastal area of Newfoundland. Journal of Fish Biology, 64: 665–679.

Dean, M. J., Hoffman, W. S., Zemeckis, D. R., and Armstrong, M. P. 2014. Fine-scale diel and gender-based patterns in behaviour of Atlantic cod (*Gadus morhua*) on a spawning ground in the Western Gulf of Maine. ICES Journal of Marine Science, 71: 1474–1489.

de Jong, K., Forland, T. N., Amorim, M. C. P., Rieucau, G., Slabbekoorn, H., and Sivle, L. D. 2020. Predicting the effects of anthropogenic noise on fish reproduction. Reviews in Fish Biology and Fisheries, 30: 245–268.

Ermolchev, V. A. 2009. Methods and results of *in situ* target-strength measurements of Atlantic cod (*Gadus morhua*) during combined trawl-acoustic surveys. ICES Journal of Marine Science, 66: 1225–1232.

Finstad, J. L., and Nordeide, J. T. 2004. Acoustic repertoire of spawning cod, *Gadus morhua*. Environmental Biology of Fishes, 70: 427–433.

Fudge, S. B., and Rose, G. A. 2009. Passive-and active-acoustic properties of a spawning Atlantic cod (*Gadus morhua*) aggregation. ICES Journal of Marine Science, 66: 1259–1263.

Garcia, H. A., Zhu, C., Schinault, M. E., Kaplan, A. I., Handegard, N. O., Godø, O. R., Ahonen, H. *et al.* 2018. Temporal–spatial, spectral, and source level distributions of fin whale vocalizations in the Norwegian Sea observed with a coherent hydrophone array. ICES Journal of Marine Science, 76: 268–283.

Gong, Z., Jain, A. D., Tran, D., Yi, D. H., Wu, F., Zorn, A., Ratilal, P. *et al.* 2014. Ecosystem scale acoustic sensing reveals humpback whale behavior synchronous with herring spawning processes and re-evaluation finds no effect of sonar on humpback song occurrence in the Gulf of Maine in fall 2006. PloS ONE, 9: e104733.

Grabowski, T. B., McAdam, B. J., Thorsteinsson, V., and Marteinsdóttir, G. 2015. Evidence from data storage tags for the presence of lunar and semi-lunar behavioral cycles in spawning Atlantic cod. Environmental Biology of Fishes, 98: 1767–1776.

Hawkins, A. 2022. The importance of sound to the Atlantic cod, *Gadus morhua*, and the Atlantic haddock, *Melanogrammus aeglefinus*. The Journal of the Acoustical Society of America, 152: 1605–1614.

Hernandez, K. M., Risch, D., Cholewiak, D. M., Dean, M. J., Hatch, L. T., Hoffman, W. S., Rice, A. N. *et al.* 2013. Acoustic monitoring of Atlantic cod (*Gadus morhua*) in Massachusetts Bay: implications

Downloaded from https://academic.oup.com/icesjms/advance-article/doi/10.1093/icesjms/fsad104/7218794 by guest on 09 August 2023

for management and conservation. ICES Journal of Marine Science, 70: 628–635.

Holt, S. A. 2008. Distribution of red drum spawning sites identified by a towed hydrophone array. Transactions of the American Fisheries Society, 137: 551–561.

Huang, W., Wang, D., Garcia, H., Godø, O. R., and Ratilal, P. 2017. Continental shelf-scale passive acoustic detection and characterization of diesel-electric ships using a coherent hydrophone array. Remote Sensing, 9: 772.

Huang, W., Wang, D., and Ratilal, P. 2016. Diel and spatial dependence of humpback song and non-song vocalizations in fish spawning ground. Remote Sensing, 8: 712.

Ingvaldsen, R. B., Gjøsæter, H., Ona, E., and Michalsen, K. 2017. Atlantic cod (*Gadus morhua*) feeding over deep water in the high Arctic. Polar Biology, 40: 2105–2111.

International Organization for Standardization. 2017. Underwater Acoustics–Terminology. Standard ISO 18405:2017(en), International Organization for Standardization, Geneva, CH. Available at: https://www.iso.org/standard/62406.html (last accessed 18 June, 2023).

Kinsler, L. E., Frey, A. R., Coppens, A. B., and Sanders, J. V. 1999. Fundamentals of Acoustics, 4th edn, pp. 560. Wiley-VCH, New Jersey.

Kleiven, A. R., Fernandez-Chacon, A., Nordahl, J.-H., Moland, E., Espeland, S. H., Knutsen, H., and Olsen, E. M. 2016. Harvest pressure on coastal Atlantic cod (*Gadus morhua*) from recreational fishing relative to commercial fishing assessed from tag-recovery data. PLoS One, 11: e0149595.

Lindholm, J., Auster, P. J., and Knight, A. 2007. Site fidelity and movement of adult Atlantic cod *Gadus morhua* at deep boulder reefs in the western Gulf of Maine, USA. Marine Ecology Progress Series, 342: 239–247.

McQueen, K., Meager, J. J., Nyqvist, D., Skjæraasen, J. E., Olsen, E. M., Karlsen, Ø., Kvadsheim, P. H. *et al.* 2022. Spawning Atlantic cod (*Gadus morhua* L.) exposed to noise from seismic airguns do not abandon their spawning site. ICES Journal of Marine Science, 79: 2697–2708.

McQueen, K., Skjæraasen, J., Nyqvist, D., Olsen, E., Karlsen, Ø., Meager, J., Kvadsheim, P. *et al.* 2023. Behavioural responses of wild, spawning Atlantic cod (*Gadus morhua* L.) to seismic airgun exposure. ICES Journal of Marine Science, 80: 1052–1065.

Makris, N. C., Godø, O. R., Yi, D. H., Macaulay, G. J., Jain, A. D., Cho, B., Gong, Z. *et al.* 2019. Instantaneous areal population density of entire Atlantic cod and herring spawning groups and group size distribution relative to total spawning population. Fish and Fisheries, 20: 201–213.

Martijn, R. L. 2021. Recreational boating interferes with the behaviour of Atlantic cod (*Gadus morhua*). PhD thesis, Institute of Marine Research, Bergen, Norway.

Meager, J. J., Skjæraasen, J. E., Fernö, A., Karlsen, Ø., Løkkeborg, S., Michalsen, K., and Utskot, S. O. 2009. Vertical dynamics and reproductive behaviour of farmed and wild Atlantic cod *Gadus morhua*. Marine Ecology Progress Series, 389: 233–243.

Meager, J. J., Skjæraasen, J. E., Karlsen, Ø., Løkkeborg, S., Mayer, I., Michalsen, K., Nilsen, T. *et al.* 2012. Environmental regulation of individual depth on a cod spawning ground. Aquatic Biology, 17: 211–221.

Midling, K., Soldal, A. V. Fosseidengen, J. E., and Øvredal, J. T. 2002. Calls of the Atlantic cod: does captivity restrict their vocal repertoire? Bioacoustics, 12: 233–235.

Mohebbi-Kalkhoran, H., Schinault, M., Makris, N. C., and Ratilal, P. 2022. Integrated computing system for real-time data processing, storage and communication with large aperture 160-element coherent hydrophone array. In OCEANS 2022, Hampton Roads. p. 1–9. IEEE.Available at: https://ieeexplore.ieee.org/document/9977064 (last accessed 18 June, 2023).

Morgan, M., DeBlois, E., and Rose, G. 1997. An observation on the reaction of Atlantic cod (*Gadus morhua*) in a spawning shoal to bottom trawling. Canadian Journal of Fisheries and Aquatic Sciences, 54: 217–223.

Nordeide, J., and Kjellsby, E. 1999. Sound from spawning cod at their spawning grounds. ICES Journal of Marine Science, 56: 326–332.

Nordeide, J. T., and Båmstedt, U. 1998. Coastal cod and north-east arctic cod-do they mingle at the spawning grounds in Lofoten? Sarsia, 83: 373–379.

Oppenheim, A. V., Willsk, A. S., and Nawab, S. H. 1997. Signals and Systems. 2nd edn. Prentice Hall, Upper Saddle River, New Jersey, London, pp. 957.

Radermacher, M.K., Schinault, M.E., Seri, S.G., and Ratilal, P., 2022. Research and design for the power hierarchy of a 160-element linear towable ocean acoustic coherent hydrophone array. In OCEANS 2022, Hampton Roads. p. 1–7. IEEE. Available at : https://ieeexplore.ieee.org/document/9977087 (last accessed 18 June, 2023).

Ratilal, P., Seri, S. G., Mohebbi-Kalkhoran, H., Zhu, C., Schinault, M., Radermacher, M., and Makris, N. C. 2022. Continental shelf-scale passive ocean acoustic waveguide remote sensing of marine ecosystems, dynamics and directional soundscapes: sensing whales, fish, ships and other sound producers in near real-time. In OCEANS 2022, Hampton Roads, pp. 1–7. IEEE. Available at : https://ieeexplore.ieee.org/document/9977054 (last accessed 18 June, 2023)

Robichaud, D., and Rose, G. A. 2004. Migratory behaviour and range in Atlantic cod: inference from a century of tagging. Fish and Fisheries, 5: 185–214.

Rousseeuw, P. J. 1987. Silhouettes: a graphical aid to the interpretation and validation of cluster analysis. Journal of computational and applied mathematics, 20: 53–65.

Rowe, S., and Hutchings, J. A. 2004. The function of sound production by Atlantic cod as inferred from patterns of variation in drumming muscle mass. Canadian Journal of Zoology, 82: 1391–1398.

Rowe, S., and Hutchings, J. A. 2006. Sound production by Atlantic cod during spawning. Transactions of the American Fisheries Society, 135: 529–538.

Schinault, M. E., Penna, S. M., Garcia, H. A., and Ratilal, P. 2019. Investigation and design of a towable hydrophone array for general ocean sensing. In OCEANS 2019—Marseille, p. 1–5. Available at: https://ieeexplore.ieee.org/document/8867239 (last accessed 18 June, 2023).

Schinault, M. E., Seri, S. G., Radermacher, M. K., Mohebbi-Kalkhoran, H., Zhu, C., Makris, N. C., and Ratilal, P. 2022. Development of a large-aperture 160-element coherent hydrophone array system for instantaneous wide area ocean acoustic sensing. In OCEANS 2022, Hampton Roads, pp. 1–9. IEEE. Available at: https://ieeexplore.ieee.org/document/9977226 (last accessed 18 June, 2023).

Sezan, M. I. 1990. A peak detection algorithm and its application to histogram-based image data reduction. Computer Vision, Graphics, and Image Processing, 49: 36–51.

Siceloff, L., and Howell, W. H. 2013. Fine-scale temporal and spatial distributions of Atlantic cod (*Gadus morhua*) on a western Gulf of Maine spawning ground. Fisheries Research, 141: 31–43.

Skjæraasen, J. E., Meager, J. J., Karlsen, Ø., Hutchings, J. A., and Fernö, A. 2011. Extreme spawning-site fidelity in Atlantic cod. ICES Journal of Marine Science, 68: 1472–1477.

Stanley, J. A., Van Parijs, S. M., and Hatch, L. T. 2017. Underwater sound from vessel traffic reduces the effective communication range in Atlantic cod and haddock. Scientific reports, 7: 1–12.

Sund, O. 1935. Echo sounding in fishery research. Nature, 135: 953–953.

Thorsteinsson, V., Pálsson, Ó. K., Tómasson, G. G., Jónsdóttir, I. G., and Pampoulie, C. 2012. Consistency in the behaviour types of the Atlantic cod: repeatability, timing of migration and geo-location. Marine Ecology Progress Series, 462: 251–260.

Tran, D. D., Huang, W., Bohn, A. C., Wang, D., Gong, Z., Makris, N. C., and Ratilal, P. 2014. Using a coherent hydrophone array for observing sperm whale range, classification, and shallow-water dive profiles. The Journal of the Acoustical Society of America, 135: 3352–3363.

Downloaded from https://academic.oup.com/icesjms/advance-article/doi/10.1093/icesjms/fsad104/7218794 by guest on 09 August 2023

Types, H. 1992. 8103, 8104, 8105, 8106: Technical documentation. Brüel & Kjær.Available at: https://www.bksv.com/-/media/literature/Product-Data/bp0317.ashx (last accessed 18 June, 2023).
Urick, R. J. 1983. Principles of underwater sound, 3rd edn. McGraw-Hill, New York.
Vester, H. I., Folkow, L. P., and Blix, A. 2004. Click sounds produced by cod (*Gadus morhua*). The Journal of the Acoustical Society of America, 115: 914–919.
Vølstad, J. H., Korsbrekke, K., Nedreaas, K. H., Nilsen, M., Nilsson, G. N., Pennington, M., Subbey, S. *et al.* 2011. Probability-based surveying using self-sampling to estimate catch and effort in Norway's coastal tourist fishery. ICES Journal of Marine Science, 68: 1785–1791.
Wang, D., Garcia, H., Huang, W., Tran, D. D., Jain, A. D., Yi, D. H., Gong, Z. *et al.* 2016a. Vast assembly of vocal marine mammals from diverse species on fish spawning ground. Nature, 531: 366.
Wang, D., Huang, W., Garcia, H., and Ratilal, P. 2016b. Vocalization source level distributions and pulse compression gains of diverse baleen whale species in the Gulf of Maine. Remote Sensing, 8: 881.
Wilson, L. J., Burrows, M., Hastie, G. D., and Wilson, B. 2014. Temporal variation and characterization of grunt sounds produced by Atlantic cod *Gadus morhua* and pollack *Pollachius pollachius* during the spawning season. Journal of fish biology, 84: 1014–1030.
Zemeckis, D. R., Dean, M. J., DeAngelis, A. I., Van Parijs, S. M., Hoffman, W. S., Baumgartner, M. F., Hatch, L. T. *et al.* 2019. Identifying the distribution of Atlantic cod spawning using multiple fixed and glider-mounted acoustic technologies. ICES Journal of Marine Science, 76: 1610–1625.
Zhu, C., Garcia, H., Kaplan, A., Schinault, M., Handegard, N., Godø, O., Huang, W. *et al.* 2018. Detection, localization and classification of multiple mechanized ocean vessels over continental-shelf scale regions with passive ocean acoustic waveguide remote sensing. Remote Sensing, 10: 1699.

Appendix

Here we examine the time series and spectrogram of reverberant cod grunt pulses and account for their form via reflection modelling. The reverberant cod grunt pulses sound like cod grunts with a ringing coda. Figure A1(a) shows a measured cod grunt with the B&K hydrophone that has a time series and spectrogram similar to typical cod grunts in the published literature (Midling *et al.*, 2002; Wilson *et al.*, 2014; Martijn, 2021). The cod grunt time series has a periodic pattern over the signal duration, with resultant spectra that are relatively discrete with multiple harmonics, following Fourier series theory (Oppenheim, 1997) for periodic signals. An example of a reverberant-sounding measured cod grunt signal is shown in Figure A1(b). It can be noticed that the periodicity is no longer present in the spectrogram, even though the signal still sounds like a cod grunt, albeit ringing effect.

Here we account for the reverberant cod grunt signals by modelling the time series and spectrogram that results when a typical cod grunt signal direct arrival undergoes coherent interference with reflected signals from the ship hull or the sea surface. Here we model the ship hull as a rigid surface with a reflection coefficient of +1 (in-phase reflection), and the sea surface as a pressure-release surface with a reflection coefficient of -1 (out-of-phase reflection). In our model, the distance between the sea surface and hydrophone is assumed to be 10 m, and the distance between fish and hydrophone is varied from 15 to 60 m. We also take into account the reduction in amplitude due to additional propagation loss and time delay experienced by the reflected signals. Two typical results are shown: the first in Figure A2(a) for a modelled cod grunt signal, including ship hull reflection, and the second in Figure A2(b) for a modelled cod grunt signal, including sea surface reflection. The measured reverberant cod grunt time series and spectra in Figure A1(b) show high similarity with the modelled reverberant cod grunt signal in Figure A2(a), where the periodicity in the time series has been altered and only the dominant harmonic is prominent in the spectrogram. This implies that the reflections from the ship hull may be the most probable cause of the reverberant cod sounds. This would occur in grunt signals from cod directly underneath our survey vessel.

The analysis here provides an explanation for the observed reverberant cod grunt signals sometimes present in our measured dataset and clarification on the time series and spectrogram structure, as well as modifications to that structure that can result when vocalizing fish are near the survey vessel or other boundaries.

Handling editor: Francis Juanes

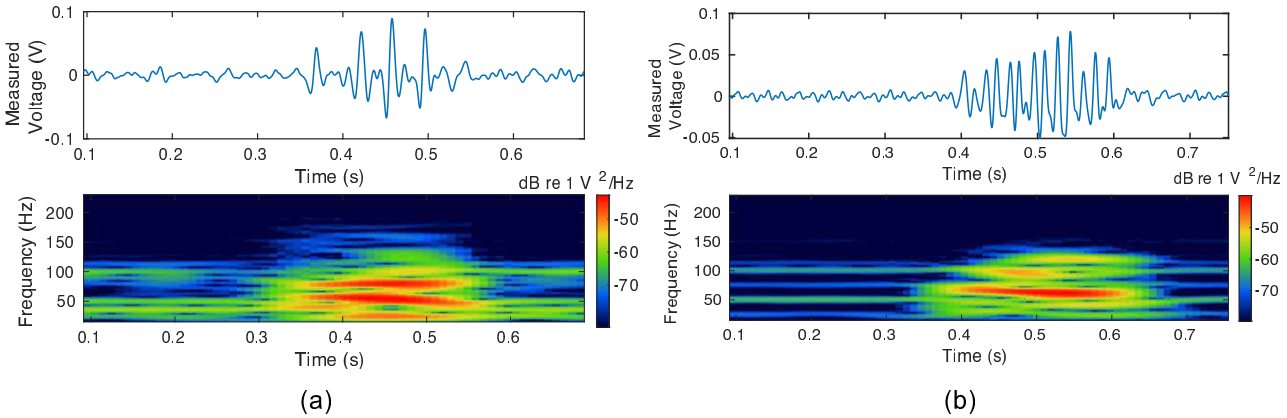

Figure A1. Measured time series and spectrogram of coastal cod grunt signals recorded on one of the pair of B&K hydrophones at (a) 17:22 PM and (b) 17:16 PM, respectively, with the hydrophone deployed vertically 10 m below RV Hans Brattstrøm on 6 March 2019. The measured signal in subplot (a) is consistent with those of a typical cod grunt and displays a periodic structure in its time series with a resulting discretized spectrum. The measured signal in subplot (b) sounds like a cod grunt but is reverberant.

Downloaded from https://academic.oup.com/icesjms/advance-article/doi/10.1093/icesjms/fsad104/7218794 by guest on 09 August 2023

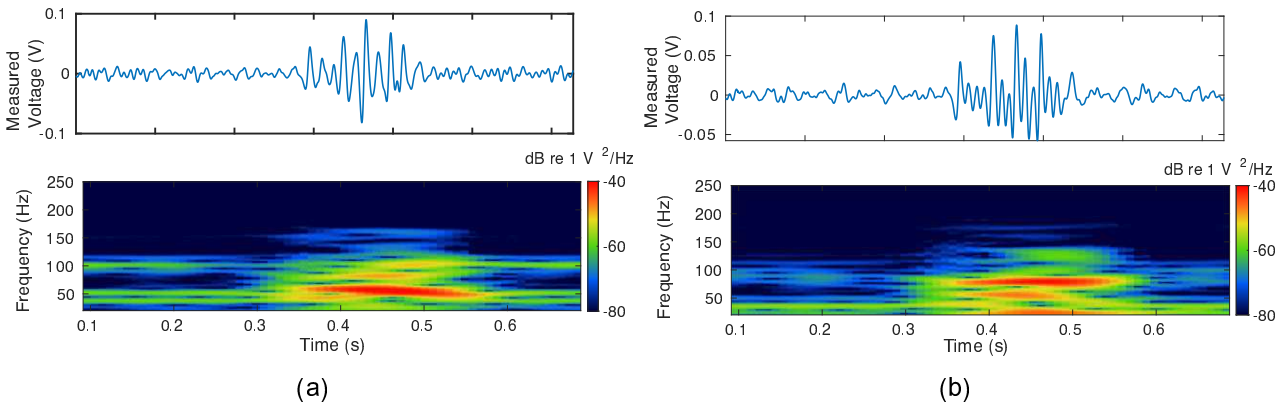

Figure A2. Modelled reverberant cod grunt signal time series and spectrogram obtained when the original cod grunt direct arrival signal from Figure A1(a) interferes coherently with reflections from (a) the ship hull and (b) the sea surface. The periodic structure present in the original time series and spectrogram in Figure A1(a) is altered significantly by reflections from the ship hull, as shown in subplot (a) here. The modelled reverberant cod grunt signal in subplot (a) here due to ship hull reflections is a good match to the measured reverberant cod grunt signal in Figure A1(b).

Downloaded from https://academic.oup.com/icesjms/advance-article/doi/10.1093/icesjms/fsad104/7218794 by guest on 09 August 2023

Received: 29 September 2022; **Revised:** 10 May 2023; **Accepted:** 25 May 2023
© The Author(s) 2023. Published by Oxford University Press on behalf of International Council for the Exploration of the Sea. This is an Open Access article distributed under the terms of the Creative Commons Attribution License (https://creativecommons.org/licenses/by/4.0/), which permits unrestricted reuse, distribution, and reproduction in any medium, provided the original work is properly cited.